Robustness, Household Heterogeneity and Business Cycles*

Edouard Djeutem Shaofeng Xu

February 13, 2023

Abstract

This paper studies the implications of model uncertainty for wealth distribution and aggregate fluctuations in a continuous time general equilibrium model. Households confront idiosyncratic income and investment risks, as well as model uncertainty that drives the risky asset return process. We find that in the presence of borrowing constraint, model distortion varies nonmonotonically with wealth, leading to non-homothetic risky asset holdings and thicker tails of the wealth distribution. An increase in investment risk induces a decline in output and wages by lowering the demand for risky capital and rebalancing household portfolio toward risk-free assets. The distributional effects of the risk shock depend on the interacting forces of model uncertainty and borrowing constraint on household's risky asset holdings.

1 Introduction

Wealth inequality has attracted extensive discussions among policy-makers and researchers in recent years. There is a broad consensus that how households allocate resources across assets is a key determinant of wealth distribution. Earlier studies have suggested that Knightian uncertainty plays an important role in understanding household portfolio choice.[1] The objective of this paper is to analyze the implications of robustness associated with risky investment for wealth distribution and aggregate fluctuations.

---

*Djeutem: Bank of Canada, djee@bankofcanada.ca. Xu: Renmin University of China, xushaofeng@ruc.edu.cn. We thank SeHyoun Ahn, Geoffrey Dunbar, Benjamin Moll, Galo Nuño, Youngmin Park, Yaz Terajima, and participants at various seminars and conferences for helpful comments and suggestions. The views expressed herein are those of the authors and not necessarily those of the Bank of Canada.

[1]This paper uses "model uncertainty" and "robustness" interchangeably, both meaning "Knightian uncertainty".

To do this, we develop a heterogeneous-agent continuous-time general equilibrium model with idiosyncratic income and investment risks. The model economy consists of infinitely-lived households composed of a worker and a producer who pool their resources to consume and save. Each producer within a household manages a firm subject to idiosyncratic investment risk; this is, in turn, owned by the household. The worker faces idiosyncratic labour productivity shocks, and supply inelastically their labour to firms. Shocks to the investment risk are the main drivers of business cycles. Households can trade two assets, including a riskless bond and a risky real asset, to smooth consumption. Borrowing is permitted but subject to a constraint. Households confront model uncertainty about the process driving the return of the risky asset and they choose robust policies *à la* Hansen and Sargent (2008). Robustness results from a dynamic zero-sum game between a household and nature. The household makes a standard consumption-portfolio choice, while nature chooses how severely to distort the risky return perceived by the household.

The starting point of our analysis is to characterize the policy functions of both poor and rich households in a stationary model without aggregate shocks. The main findings are three-fold. First, the size of model distortion chosen by nature varies nonmonotonically with household wealth, reaching its maximum at some intermediate wealth level. Nature finds it optimal not to distort heavily the perceived risky return of poor households as they hold little risky asset due to the borrowing constraint. For households in possession of large wealth, the nature's benefit from twisting their perception of the risky return is insignificant so the distortion is also small. Second, we formulate the effects of model uncertainty on the speed at which the wealth of unlucky households hits the borrowing constraint. It is shown that under certain conditions, robustness accelerates the speed of convergence. Model uncertainty discourages these households from investing in the risky asset due to their mistrust of the probability distribution underlying the risky return process. Lower wealth translates into a tighter borrowing constraint which further constrains their investment in the risky asset. These two forces together leads to a slower wealth accumulation. Third, we derive the policy functions of the rich. For these households, the wealthier they are, the less nature distorts their perception, and thus the smaller is the reduction in the proportion of their wealth invested in the risky asset. In other words, robustness makes richer households even richer.

To illustrate the aggregate and distributional implications of model uncertainty, we calibrate the model to the U.S. economy. We choose the robustness parameter by the detection error probability in line with the practice in the literature. Most notably, the parameterized stationary model thickens both tails of the wealth distribution that improves the model's fit to the U.S. wealth distribution data. In order words, we match not only the wealth share of the bottom 50 percent but also that of the top 1. This extends the existing models in the literature that usually rely on a multiple combination of mechanisms to match both tails of the distribution.

We find that an increase in investment risk induces a decline in output and wages by lowering the demand for risky capital. Households thus rebalance their portfolio toward risk free assets leading to aggregate overaccumaltion of these assets and a sharp drop in the required risk free rate necessary to clear the bond market. Consumption rises counterfactually compared to a standard recession as the decline in interest rate makes savings less attractive. Model uncertainty related to the risky capital returns process magnifies each of the above mechanism by further depressing risky capital demand which takes longer to rebuild. Model uncertainty thus generates a slower recovery from the investment risk shock.

Moreover, the shock brings about rich distributional ramifications due to the nonhomethetic behavior of model uncertainty on risky capital holdings and the presence of borrowing constraint. In response to an investment risk shock wealth-rich households lose the most because they are the primary capital holder in the economy. As such, their portfolio reallocation toward risk free assets is the strongest. Households seating at the middle of the wealth distribution, by contrast, take advantage of the high private equity premium engineered by low interest rate to lever up and increase their exposure to risk capital. For wealth-poor households, the equilibrium change in prices following an increase in investment risk is important. Decreasing wages trigger a depletion of human wealth which constitute a larger fraction of their total wealth. These households liquidate their capital but increase their bond borrowing in low interest environment generated by the aggregate flight to safety.

Our paper is related to three strands of the literature. First, it is connected to the literature that examines the effects of model uncertainty on households consumption-portfolio choice and the macroeconomy. Examples include Anderson et al. (2003), Maenhout (2004), Luo et al. (2020), and Kasa and Lei (2018).[2] Recent work by Kasa and Lei (2018) is the study closest to ours. The current paper differs from theirs in the following two aspects. First, we bring to attention the interactions between model uncertainty and borrowing constraint. To our best knowledge, this is the first paper that characterizes this interplay explicitly, which bears important macroeconomic implications. For example, borrowing constraint changes the outcome of the dynamic zero-sum game, resulting in a nonmonotonic relationship between model distortion and wealth. By contrast, the relationship is monotonic in Kasa and Lei (2018). Second, their paper answers the question

[2]Empirical studies, e.g., Dimmock et al. (2016) and Brenner and Izhakian (2018), provide supporting evidence for the importance of Knightian uncertainty for understanding household portfolio choice.

of whether model uncertainty can explain the rise in top wealth shares in the U.S., while our main goal is to analyze the effects of robustness on the whole wealth distribution and evaluate its business cycles implications.

The current paper also contributes to the growing literature that analyzes the macroeconomic effects of household heterogeneity in continuous time.[3] Examples include Benhabib et al. (2016), Gabaix et al. (2016), Achdou et al. (2022), Cao and Luo (2017), Kaplan et al. (2018), Nuno and Moll (2018), and Toda and Walsh (2020). Our paper is most closely related to Achdou et al. (2022), upon which we build our model. The paper brings two contributions to this literature. First, we show that robustness provides a useful perspective for understanding both tails of wealth distribution. Second, we extend relevant results in Achdou et al. (2022) for the context of model uncertainty, and derive a novel formulation for its impact on the speed of convergence.

Finally, the paper is related to a few studies that employ representative agent models in which stochastic volatility and model uncertainty drive business cycles. Stochastic volatility shock associated with a TFP generates a typical recession in these models accompanied by a decline consumption, investment, output and hours (Bidder and Smith, 2012; Backus et al., 2015). However, these models fail to account for magnitudes and persistence of shocks and robustness usually has a small effect on business cycles quantities. Di Tella and Hall (2022) offer a two-agents stochastic growth model where idiosyncratic investment risk rises in recessions and drives risk premium up. Firm responds by cutting down risky labour demand which lead to contractions in consumption, investment, output and hours in general equilibrium. Our contribution is to provide a distinct rationale for a recession, one that puts the non-homothetic portfolio choice in presence of borrowing constraint and idiosyncratic investment risk at the center stage.

The rest of the paper is structured as follows. Section 2 describes the model. Section 3 characterizes the policy functions of both poor and rich households. Section 4 present our parametrization and numerical computation strategies. In section 5, we examine the results of our numerical experiments. Section 6 concludes.

2 The Model

This section constructs a continuous-time general equilibrium economy populated by a continuum of infinitely-lived households. Each household consists of a worker and a

[3]There is also a large literature that studies equilibrium models with heterogenous households in discrete time. Examples include Bewley (1986), Huggett (1993), Aiyagari (1994), Benhabib et al. (2015), Quadrini and Ríos-Rull (2015) and references therein.

producer (or entrepreneur). The worker supplies his labor endowment inelastically to the labor market. The entrepreneur runs a privately-held firm that hires labor in a competitive labor market and employs capital accumulated by its household owner. Households face aggregate volatility shocks and idiosyncratic labor and capital income shocks. They can save in a riskless bond and invest risky real capital in the firm they own.

2.1 Preferences

Households have standard preferences over consumption as

$$U_0 = \mathbb{E}_0 \left[\int_0^{+\infty} e^{-\rho t} u(c_t) dt \right], \tag{2.1}$$

where ρ denotes the subjective discount factor and c_t the consumption at date t. The periodic utility function $u(c)$ is specified to be of the form

$$u(c) = \frac{c^{1-\gamma}}{1-\gamma}, \ \gamma > 0. \tag{2.2}$$

2.2 Endowment and technology

Each worker is endowed with one unit of labor, whose productivity z_t evolves stochastically over time. The productivity follows a two-state Poisson process and takes values in $\{z_1, z_2\}$ with $z_1 < z_2$. The process switches from state 1 to state 2 with intensity λ_1 and from state 2 to state 1 with intensity λ_2.

Households also receive capital income from their own private firm. Each firm produces output using a Cobb-Douglas technology

$$y_t = F(k_t, l_t) = k_t^{\alpha} l_t^{1-\alpha}, \tag{2.3}$$

where α is the capital share, k_t denotes the private capital, and l_t stands for the labour hired at the wage rate w_t. Firm profit or household capital income is subject to idiosyncratic shocks, and it evolves according to

$$d\varpi_t = (y_t - w_t l_t - \delta k_t) dt + \sqrt{\vartheta_t} k_t dW_t, \tag{2.4}$$

where δ is the rate of capital depreciation, and W_t is a standard Brownian motion representing an idiosyncratic shock to the capital income. The capital income shock is independent and identically distributed across firms and time, and can be interpreted as a stand-in for any type of exogenous idiosyncratic risk in the returns to private investment.

The variance ϑ_t of the idiosyncratic capital income shocks fluctuates over time, driven by an economic-wide risk shock. We assume ϑ_t follows a Cox-Ingersoll-Ross process:[4]

$$d\vartheta_t = \theta \left(\bar{\vartheta} - \vartheta_t\right) dt + \nu \sqrt{\vartheta_t} dB_t, \tag{2.5}$$

where θ, $\bar{\vartheta}$, and ν are positive parameters, denoting, respectively, the mean-reverting rate, the mean volatility level, and the volatility of volatility. In equation (2.5), B_t is a standard Browninan motion that captures the aggregate volatility risk in the economy, and serves as the only exogenous driver of business cycles. It is assumed that aggregate and idiosyncratic shocks are independently distributed, so the paper focuses on connections between volatility shocks and economic activity that arise through the model's internal economic structure rather than through purely statistical channels between different types of shocks. In the model, each firm chooses employment after the capital stock has been installed and the contemporaneous shocks have been observed.

2.3 Market structure

Households use two types of assets to smooth consumption. First, they have an access to an instantaneously maturing riskless bond b_t that pays an interest rate r_t. They can save or borrow in the bond subject to a borrowing constraint

$$b_t \geq -\phi, \tag{2.6}$$

where $\phi > 0$. Households can also invest real risky capital k_t in their own private firm. The associated capital return $d\tilde{R}_t = d\varpi_t / k_t$ varies over time as

$$d\tilde{R}_t = R_t dt + \sqrt{\vartheta_t} dW_t, \tag{2.7}$$

where R_t is the unknown expected capital return. Capital cannot be negative, i.e., $k_t \geq 0$. Denote $a_t = b_t + k_t$ as a household's net worth. The borrowing constraint and the requirement of non-negative holdings of the risky capital can be summarized as

$$0 \leq k_t \leq a_t + \phi, \tag{2.8}$$

where $a_t \geq \underline{a} = -\phi$ is the constraint imposed on net worth.

[4]Apart from its analytical tractability, the process (2.5) has been broadly adopted in finance to capture the dynamics of stock price volatility, one important measure of macroeconomic uncertainty proposed by the existing literature of uncertainty shocks, and thus is a reasonable volatility specification.

The dynamics of the net worth of a household are given by

$$\begin{aligned} da_t &= z_t w_t dt + k_t d\tilde{R}_t + b_t r_t dt - c_t dt \\ &= \Big(z_t w_t + r_t a_t + \hat{\pi}_t k_t - c_t \Big) dt + \sqrt{\vartheta_t} k_t dW_t \\ &= \hat{s}(a_t, z_t, G_t, \vartheta_t) dt + \sqrt{\vartheta_t} k_t dW_t \end{aligned} \tag{2.9}$$

where $\hat{\pi}_t = R_t - r_t$ is the excess return of the risky capital and G_t is the cross-sectional distribution of households along networth a_t and productivity z_t at date t.

2.4 Robust portfolio choice

In this economy, households do not perfectly know the probability measure underlying the idiosyncratic capital income shocks in the risky return process (2.7). We capture this model uncertainty using the notion *à la* Hansen et al. (2006) and Hansen and Sargent (2008).[5] When making their consumption-portfolio decisions, households consider multiple alternative probability measures and choose policies to obtain the highest expected utility under the worst case scenario. Robustness is achieved by assuming that each household plays a zero-sum game with nature. Nature distorts the drift term of the risky return process, while the household makes its portfolio choice taking the distorted return as given.

More precisely, let q^0 be a probability measure defined by the Brownian motion in the reference law of motion describing return process (2.7) and q an alternative law. The distance between the two laws is measured by the expected discounted log likelihood ratio also called relative entropy

$$\mathcal{R}(q) = \rho \int_0^\infty e^{-\rho t} \left[\int \log \left(\frac{dq_t}{dq_t^0} \right) dq_t \right] dt = \frac{1}{2} \mathbb{E}_0 \left[\int_0^\infty e^{-\rho t} h_t^2 dt \right], \tag{2.10}$$

where the second equality is due to the Girsanov Theorem and h_t is a square integrable and measurable process. The value of h_t represents the distortion chosen by nature. One can then view the alternative model q as induced by the following Brownian motion

$$d\tilde{W}_t = dW_t - h_t dt. \tag{2.11}$$

[5] For the axiomatic foundations of model uncertainty, please refer to Gilboa and Schmeidler (1989), Maccheroni et al. (2006), and Strzalecki (2011).

Consequently, the alternative risky return process is

$$d\tilde{R}_t = \left(R_t + \sqrt{\vartheta_t} h_t\right) dt + \sqrt{\vartheta_t} d\tilde{W}_t. \tag{2.12}$$

As a result, the dynamic budget constraints perceived by a household can be written as

$$\begin{aligned} da_t &= \left(z_t w_t + r_t a_t + \pi_t k_t - c_t\right) dt + \sqrt{\vartheta_t} k_t d\tilde{W}_t \\ &= s(a_t, z_t, G_t, \vartheta_t) dt + \sqrt{\vartheta_t} k_t d\tilde{W}_t \end{aligned} \tag{2.13}$$

where $\pi_t = R_t - r_t + \sqrt{\vartheta_t} h_t = \hat{\pi}_t + \sqrt{\vartheta_t} h_t$ represents the perceived excess return.

The objective of a household is to choose a consumption plan $\{c_t\}$ and an investment plan in the risky asset $\{k_t\}$ to maximize its lifetime utility, subject to budget constraint (2.13) and borrowing constraint (2.8). By contrast, nature chooses a distortion plan $\{h_t\}$ to minimize a distortion cost represented by the relative entropy $\mathcal{R}(q)$.[6] Mathematically, the robust consumption-portfolio choice problem can be formulated as

$$\begin{aligned} &\max_{\{c_t, k_t\}} \min_{\{h_t\}} \mathbb{E}_0 \int_0^\infty e^{-\rho t} \left(\frac{c_t^{1-\gamma}}{1-\gamma} + \frac{1}{2\varepsilon} h_t^2 \right) dt \\ &\text{s.t. } \; da_t = s(a_t, z_t, G_t, \vartheta_t) dt + \sqrt{\vartheta_t} k_t d\tilde{W}_t \\ &\qquad 0 \le k_t \le a_t + \phi. \end{aligned} \tag{2.14}$$

The parameter ε represents the robustness parameter, where $1/\varepsilon$ can be interpreted as a marginal cost of distorting the drift term of the risky return process. When $\varepsilon = 0$, the marginal cost is infinite and nature chooses $h = 0$ so that there is no doubt in the law of motion of the risky return. In this case, the model reduces to a standard Merton portfolio choice problem without robustness.

2.5 Recursive equilibrium

A recursive equilibrium consists of wage $w(G, \vartheta)$, capital return $R(G, \vartheta)$, interest rate $r(G, \vartheta)$, value function $v(a, z_j, G, \vartheta)$, optimal consumption $c(a, z_j, G, \vartheta)$, optimal investment in the risky capital $k(a, z_j, G, \vartheta)$, optimal distortion $h(a, z_j, G, \vartheta)$, and density function $g_t(a, z_j)$ such that

1. The value function and policy functions solve the optimization problem (2.14).

[6] This form of cost functions has been used widely in the literature, e.g., Hansen and Sargent (2008).

2. The density function $g_{t,j}(a)$ satisfies the Kolmogorov Forward (KF) equation:

$$\frac{\partial}{\partial t} g_{t,j}(a) = -\frac{\partial}{\partial a}\left(\hat{s}(a, z_j, G_t, \vartheta_t) g_{t,j}(a)\right) - \lambda_j g_{t,j}(a) + \lambda_{-j} g_{t,-j}(a) + \frac{1}{2}\frac{\partial^2}{\partial a^2}\left(\vartheta k^2 g_{t,j}(a)\right), \tag{2.15}$$

where $g_{t,j}(a) = g_t(a, z_j)$ with j denoted as one state of income and $-j$ as the other.

3. The bond market clears:

$$\sum_{j=1}^{2} \int (a - k) g_t(a, z_j) = 0. \tag{2.16}$$

4. The labor market clears:

$$\sum_{j=1}^{2} \int z_j g_t(a, z_j) = 1. \tag{2.17}$$

3 Equilibrium characterization

This section characterizes the equilibrium dynamics of macroeconomic aggregates, and more importantly, the impacts of model uncertainty on the consumption-investment behavior of households. The analysis provides important insights on the implications of robustness for wealth distribution and aggregate fluctuations.

Proposition 1. *In equilibrium, the wage and the expected capital return satisfy*

$$w_t = w(K_t, \vartheta_t) = (1-\alpha)K_t^{\alpha}, \; R_t = R(K_t, \vartheta_t) = \alpha K_t^{\alpha-1} - \delta, \tag{3.1}$$

where $K_t = \sum_{j=1}^{2} \int k g_t(a, z_j)$ denotes the aggregate capital stock and its evolution follows

$$dK_t = (K_t^{\alpha} - \delta K_t - C_t)\, dt, \tag{3.2}$$

with $C_t = \sum_{j=1}^{2} \int c g_t(a, z_j)$ being the aggregate consumption in equilibrium.

We now characterize the individual behavior of households across the wealth distribution. The characterization deploys a perturbation method related to the distortion parameter ε, which allows us to disentangle the effects of robustness in an analytical fashion. To derive economic intuition, the remainder of the section focuses the analysis on the consumption-investment decisions in the steady state.

Denote w, R and r as the steady-state wage, expected capital return and risk-free rate, respectively, and $\sigma = \sqrt{\vartheta}$ as the stationary standard deviation of capital income shocks. In the steady state, the household's optimization problem (2.14) can be summarized by the following Hamilton-Jacobi-Bellman (HJB) equation:

$$\rho v_j(a) = \max_{c,0\le k\le a+\phi} \min_h \left\{ \begin{array}{c} u(c) + \frac{1}{2\varepsilon}h^2 + v_j'(a)(wz_j + ra + (R+\sigma h - r)k - c) \\ +\frac{1}{2}v_j''(a)\sigma^2 k^2 + \lambda_j(v_{-j}(a) - v_j(a)) \end{array} \right\}, j = 1,2 \tag{3.3}$$

which is solved by value function $v_j(a)$ and policy functions $c_j(a)$, $k_j(a)$ and $h_j(a)$. The associated first-order conditions are

$$\begin{aligned} u'(c_j(a)) &= v_j'(a) \\ k_j(a) = \min\left\{-\frac{\pi}{\sigma^2}\frac{v_j'(a)}{v_j''(a)}, a+\phi\right\} &= \min\left\{\frac{R-r}{\sigma^2}\frac{v_j'(a)}{\varepsilon(v_j'(a))^2 - v_j''(a)}, a+\phi\right\} \\ h_j(a) &= -\varepsilon\sigma k_j(a) v_j'(a), \end{aligned} \tag{3.4}$$

where households use perceived excess return π instead of actual one $\hat{\pi}$ to choose capital. For the sake of notational convenience, we use $v_{j,0}(a)$, $c_{j,0}(a)$ and $k_{j,0}(a)$ to denote the corresponding value function and policy functions in an otherwise identical economy without model uncertainty, i.e., they represent the solution to equation (3.3) with $\varepsilon = 0$.

We first consider the saving behavior of wealth-poor households, with the results summarized in the following proposition.

Proposition 2. *Suppose that $r < \rho$ at the steady state with $\underline{a} > -\frac{wz_1}{r}$. As $a \to \underline{a}$, the following hold:*

1. *The robust saving function $s_j(a)$ satisfies:*

$$s_1(a) \sim -\sqrt{2\varsigma_1(a - \underline{a})}, \tag{3.5}$$

where ς_1 is a constant defined by

$$\begin{aligned} \varsigma_1 = & \frac{(\rho - r)c_1(\underline{a})}{\gamma} + \lambda_1(c_2(\underline{a}) - c_1(\underline{a})) \\ & -\frac{c_1(\underline{a})}{2\gamma}\left(\frac{R-r}{\sigma}\right)^2\left(\frac{\gamma+1}{\gamma} - \frac{1}{\gamma}\frac{c_1(\underline{a})c_1''(\underline{a})}{c_1'(\underline{a})^2}\right)\left(1 - 2\frac{\varepsilon}{\gamma}\frac{c_1(\underline{a})^{1-\gamma}}{c_1'(\underline{a})}\right). \end{aligned} \tag{3.6}$$

2. *The realized saving function $\hat{s}_j(a)$ satisfies:*

$$\hat{s}_1(a) \sim -\sqrt{2\hat{\varsigma}_1(a - \underline{a})}, \tag{3.7}$$

where $\hat{\varsigma}_1$ is a constant defined as

$$\hat{\varsigma}_1 = \varsigma_1 - \lambda\varepsilon \tag{3.8}$$

with the coefficient

$$\lambda = \frac{c_1(\underline{a})}{\gamma}\left(\frac{R-r}{\sigma}\right)^2\left(\frac{\gamma+1}{\gamma} - \frac{1}{\gamma}\frac{c_1(\underline{a})\,c_1''(\underline{a})}{c_1'(\underline{a})^2}\right)\left(\frac{c_1(\underline{a})^{1-\gamma}\,c_1'(\underline{a})}{(\gamma+1)\,c_1'(\underline{a})^2 - c_1''(\underline{a})\,c_1(\underline{a})}\right). \tag{3.9}$$

Part 1 of Proposition 2 characterizes the shape of the robust saving function of low income households in the proximity of the borrowing constraint, where the function behaves like $-\sqrt{\varsigma_1(a-\underline{a})}$. As shown in (3.6), the value of ς_1 is determined by three different factors. The first and second terms on the right-hand side of the equation capture respectively the effects of intertemporal substitution and income uncertainty, whereas the third represents the impact from risky investment taking robustness concerns into consideration.

Notwithstanding households make their portfolio choice based on the perceived return process given in (2.12), their actual wealth accumulation is driven by the realized return and thus the realized saving function $\hat{s}_j$. As characterized in Part 2 of Proposition 2, the function exhibits a similar square-root shape, where the parameter $\hat{\varsigma}_1$ measures the speed of convergence to the borrowing constraint.[7] If $c_1' > 0$ and $c_1'' \leq 0$, i.e., the consumption function is increasing and concave with respect to wealth, one can deduce from (3.9) that $\lambda > 0$ and thus $\hat{\varsigma}_1 < \varsigma_1$ by (3.8). Intuitively speaking, because the realized return from the risky asset is higher than what would be perceived by a household with robustness concerns, its actual wealth grows at a rate faster than perceived. As such, the pace of hitting the borrowing constraint due to successive low-income realizations is slower than what it would be based on the robust saving function.

To identify the impact of model uncertainty on the saving behavior of wealth-poor households, we compare our benchmark economy to an otherwise identical economy without robustness by evaluating the disparity between their respective speeds of convergence to the borrowing constraint.[8] The results are presented in the following proposition, whose proof relies on a first-order Taylor expansion of $\hat{\varsigma}_1$ around $\varepsilon = 0$,

Proposition 3. *Suppose that $r < \rho$ at the steady state with $\underline{a} > -\frac{wz_1}{r}$. Denote $c_j(a) = c_{j,0}(a) + \varepsilon c_{j,1}(a) + O(\varepsilon^2)$, $j = 1, 2$, as the first-order approximation of the consumption function, where*

[7] It is straightforward to show that the wealth of a household with initial wealth a_0 above $\underline{a}$ and successive draws of low-income state z_1 hits the borrowing constraint in finite time $T = \sqrt{\frac{2(a_0-\underline{a})}{\hat{\nu}_1}}$.

[8] This comparative analysis is in essence a partial equilibrium study by abstracting away the general equilibrium effects of robustness on prices.

$c_{j,0}(a)$ represents the consumption function in the economy without robustness. It holds that

$$\hat{\varsigma}_1 \approx \varsigma_{1,0} + \varsigma_{1,1}\varepsilon, \tag{3.10}$$

where $\hat{\varsigma}_1$ is the speed of convergence in the benchmark economy as given in (3.8),

$$\varsigma_{1,0} = \frac{(\rho - r)c_{1,0}\left(\underline{a}\right)}{\gamma} + \lambda_1\left(c_{2,0}\left(\underline{a}\right) - c_{1,0}\left(\underline{a}\right)\right) - \frac{c_{1,0}\left(\underline{a}\right)}{2\gamma}\left(\frac{R-r}{\sigma}\right)^2\left(\frac{\gamma+1}{\gamma} - \frac{1}{\gamma}\frac{c_{1,0}\left(\underline{a}\right)c''_{1,0}\left(\underline{a}\right)}{c'_{1,0}\left(\underline{a}\right)^2}\right) \tag{3.11}$$

represents the counterpart of $\hat{\varsigma}_1$ in the economy without robustness, and $\varsigma_{1,1}$ is some constant defined in the Appendix A.

In a similar vein to (3.7), as $a \to \underline{a}$ the saving function of income-poor households in the economy without model uncertainty approximately equals

$$s_{1,0}\left(a\right) \sim -\sqrt{2\varsigma_{1,0}\left(a - \underline{a}\right)}, \tag{3.12}$$

where $\varsigma_{1,0}$ is given in (3.11). The ensuing proposition identifies a set of sufficient conditions that enables a comparison of $\hat{s}_1(a)$ and $s_{1,0}(a)$ near the borrowing constraint.

Proposition 4. *Suppose that $r < \rho$ at the steady state with $\underline{a} > -\frac{wz_1}{r}$. If the following three conditions are satisfied:*

1. $c_{2,1}\left(\underline{a}\right) > c_{1,1}\left(\underline{a}\right) > 0$;
2. $c'_{1,0}(a) > 0$ *and* $c''_{1,0}(a) < 0$;
3. $\theta(\underline{a}) < 0$, *where $\theta(a)$ is a function defined in the Appendix A,*

it holds that

$$\hat{\varsigma}_1 > \varsigma_{1,0}, \tag{3.13}$$

and there exists an $\epsilon > 0$ such that for $a \in \left(\underline{a}, \underline{a} + \epsilon\right)$,

$$\hat{s}_1(a) < s_{1,0}(a) < 0. \tag{3.14}$$

Proposition 4 says that near the borrowing constraint households in the benchmark economy dissave at a faster rate than in the economy without robustness, and they are also more susceptible to becoming credit constrained following negative income shocks. This result is driven by two forces. First, robustness induces households to believe that the excess return on the risky asset is lower than what it is in reality. Consequently, they invest less in the higher yielding asset, which decelerates their wealth accumulation. Second, lower wealth translates into a tighter borrowing constraint in (2.8). This collateral effect further discourages the investment in the risky private capital. By implication, ceteris paribus, robustness concerns associated with the idiosyncratic investment risk tend to increase the mass of households on the left tail of the wealth distribution.

We now proceed to analyze the consumption-investment behavior of wealth-rich households. We first derive an auxiliary lemma concerning a homogeneity property of the value function defined in (3.3). This property is also instrumental for handling boundary conditions in the subsequent numerical analysis.

Lemma 1. *As $a \to \infty$, the value function solving the HJB equation (3.3) can be approximately written as*

$$v_j(a) \approx v_{j,0}(a) + \varepsilon v_{j,1}(a), \tag{3.15}$$

where the two functions $v_{j,0}(a)$ and $v_{j,1}(a)$ are such that for any $\xi > 0$,

$$v_{j,0}(\xi a) = \xi^{1-\gamma} v_{\xi,j,0}(a), \; v_{j,1}(\xi a) = \xi^{2(1-\gamma)} v_{\xi,j,1}(a), \tag{3.16}$$

with $v_{\xi,j,0}(a)$ and $v_{\xi,j,1}(a)$ satisfying two functional equations defined in the Appendix A.

The following proposition provides an analytical approximation for the policy functions when wealth is very large. The proof rests on the fact that borrowing constraint and labor income become irrelevant for the portfolio choice of rich households.

Proposition 5. *As $a \to \infty$, the individual policy functions solving the HJB equation (3.3) can be approximately written as*

$$\begin{aligned} c_j(a) &\approx c_{j,0}(a) + \varepsilon c_{j,1}(a) = \alpha_0^{-\frac{1}{\gamma}} a - \varepsilon \frac{1}{\gamma} \alpha_0^{-\frac{1}{\gamma}-1} \alpha_1 a^{2-\gamma} && (3.17) \\ k_j(a) &\approx k_{j,0}(a) + \varepsilon k_{j,1}(a) = \frac{R-r}{\gamma\sigma^2} a - \varepsilon \frac{R-r}{\sigma^2} \frac{\alpha_0^2 + \alpha_1(\gamma-1)}{\alpha_0 \gamma^2} a^{2-\gamma} && (3.18) \\ h_j(a) &\approx -\varepsilon \frac{R-r}{\gamma\sigma^2} \alpha_0 a^{1-\gamma}, && (3.19) \end{aligned}$$

where α_0 is given by (A.69) and α_1 by (A.72) in the appendix.

As evidenced in Lemma 1 and Proposition 5, robustness concerns also induce deviations in consumption-investment behavior of rich households from the standard Merton solution, which is represented by value function $v_{j,0}(a)$ and policy functions $c_{j,0}$ and $k_{j,0}$.[9]

[9] Kasa and Lei (2018) derive similar robust policy functions in a Blanchard–Yaari framework over the entire state space. In our paper, these functions are only valid for the rich and they take a different shape in the left tail due to the borrowing constraint.

The proposition shows that if $\gamma > 1$ and $\alpha_1 > 0$, the presence of robustness concerns decreases the consumption and risk investment of rich households, with the size of model distortion declining with wealth and diminishing to zero as wealth approaches infinity.

This monotonic relationship between distortion and wealth, however, does not extend to the whole spectrum of the wealth distribution, as shown by the following proposition.

Proposition 6. *Suppose that $r < \rho$ at the steady state with $\underline{a} > -\frac{wz_1}{r}$. The optimal distortion function satisfies: for $\gamma > 1$,*

$$\lim_{a \to \underline{a}} h_j(a) = \lim_{a \to \infty} h_j(a) = 0, \tag{3.20}$$

and there exists an $a_j^* \in (\underline{a}, \infty)$ such that

$$h_j'(a_j^*) = 0. \tag{3.21}$$

Proposition 6 summarizes the effects of wealth on the way nature distorts the return of the risky private capital. By (2.12), the distortion alters the drift of the perceived risky return process from R to $R + \sigma h_j(a)$. As shown in (3.4), the size of distortion equals

$$h_j(a) = -\varepsilon \sigma k_j(a) v_j'(a), \tag{3.22}$$

which is a function of a household's holding of private capital $k_j(a)$ and its marginal utility of wealth $v_j'(a)$. Nature does not distort the risky return perceived by constrained households, because they do not hold any private capital $k_j(a) = 0$ thanks to the borrowing constraint in (2.8) and then have nothing to lose. By contrast, if the value function $v_j(a)$ is concave, rich households tend to have a small marginal utility of wealth $v_j'(a)$. When the decrease in the marginal utility overshadows the increase in the holding of private capital as wealth becomes sufficiently large, the impact of model uncertainty dissipates. Intuitively, wealth discourages nature from distorting the risky return because the more wealth a household holds, the less pessimistic the household is about the return obtained from the private investment. By implication, the maximal distortion occurs at some intermediate wealth level a_j^* as defined in (3.21), suggesting a likely U-shaped relation between distortion and wealth across the wealth spectrum. This result is in a stark contrast to the literature, such as Kasa and Lei (2018), which argues that model distortion depends negatively on wealth globally. The non-monotonic relation revealed herein manifests the importance of financial constraints for the game between households and nature.

We conclude this section by comparing in Figure 1 the policy function $x_j(a)$ in the benchmark economy with its counterpart $x_{j,0}(a)$ in an otherwise identical economy ab-

Figure 1: The effects of robustness on policy functions

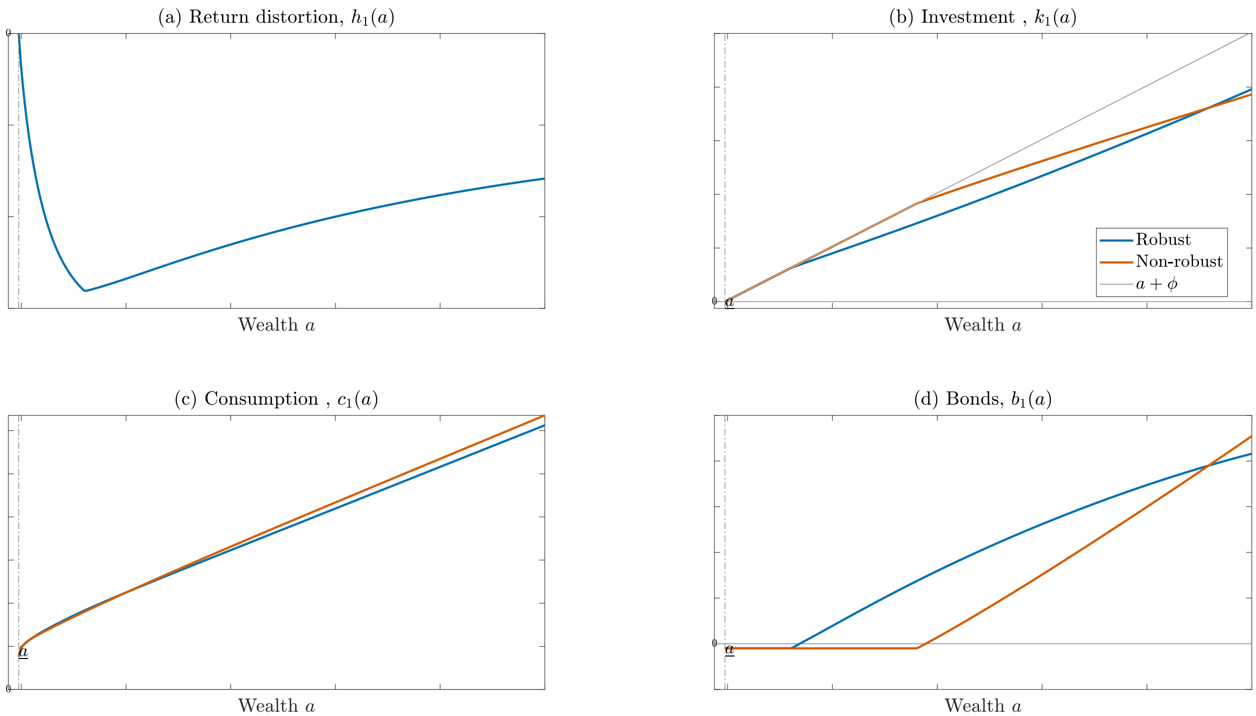

sent model uncertainty. Panel (a) shows that the size of distortion displays a U-shaped relation with wealth, which is consistent with the preceding discussions. Panel (b) indicates that robustness concerns reduce the risky investment across the board. The reduction, however, varies non-monotonically with wealth, and it resembles closely the behavior of the distortion. Panel (c) portrays the implications of model uncertainty for consumption. Robustness reduces the risky investment of households near the borrowing constraint, resulting in an increase in their consumption. Contrarily, the consumption of the rich falls as a result of a reduction in net worth thanks to the decrease in their holdings of the higher yielding capital. Panel (d) depicts the reaction of saving to robustness. The ratio is above one for the low-income state and below one for the high-income state. Because saving is negative in the low-income state and positive in the high-income state, it suggests that the preference for robustness decelerates wealth accumulation.

4 Calibration and computation

This section parameterizes the benchmark model and describes the numerical algorithm for solving the recursive equilibrium.

4.1 Calibration

The model is parameterized according to U.S. data. For parameters describing preferences, we set the subjective discount rate ρ at 0.055 to match an average annual real interest rate of 4 percent. The risk aversion γ is fixed at 2, a value well within the consensus range of the parameter.

The parameters governing the idiosyncratic two-state productivity process are estimated as follows. We interpret state 1 as unemployment and state 2 as employment. Accordingly, we choose the transition probabilities $\lambda_1 = 0.986$ and $\lambda_2 = 0.052$ to reproduce the long-run average unemployment rate of 5 percent and the job finding rate of 0.986 in line with Blanchard and Galí (2010). The corresponding labor productivities are set at $z_1 = 0.72$ and $z_2 = 1.015$, so that productivity in state 1 is about 71 percent of that in state 2 as in Hall and Milgrom (2008), and the average productivity equals one.

There are no precise estimates of the level of idiosyncratic investment risk because of a lack of sufficiently rich data about entrepreneurial returns, as argued for example in Moskowitz and Vissing-Jørgensen (2002). In the baseline parametrization, we follow Angeletos (2007) by setting $\sigma = \sqrt{\bar{\vartheta}}$ at 0.125, a conservative estimate of the risk in the U.S. Capital depreciates at rate $\delta = 0.08$ and the share of capital in production is $\alpha = 0.36$, both of which are standard in the literature. The values of the persistence and the volatility of risk shocks are taken from Di Tella and Hall (2022) and set at $\theta = 0.2$ and $\nu = 0.16$.

Table 1: Baseline parameterization

	Parameter	Value
Subjective discount rate	ρ	0.055
Relative risk aversion	γ	2
Robustness parameter	ε	0.3
Borrowing limit	ϕ	0.5
Income jump	λ_1,λ_2	0.986, 0.052
Low income	z_1	0.72
High income	z_2	1.015
Volatility risky return	σ	0.125
Depreciation rate	δ	0.08
Capital share	α	0.36
stoc vol persistence	θ	0.20
stoc vol volatitlity	ν	0.16

The borrowing constraint parameter ϕ, which affects the fraction of households holding negative wealth and the overall wealth concentration, is pinned down at 0.5. The value is broadly in line with Huggett (1993) and Achdou et al. (2022). We calibrate the robustness parameter ε based on a methodology similar to Anderson et al. (2003) and Kasa and Lei (2018), and set it at 0.3. The corresponding dependent detection error probabilities are all above 44 percent, suggesting the empirical plausibility of model uncertainty.

The performance of the parameterized benchmark model is evaluated by comparing the model's implications for wealth distribution with their respective data counterparts. Table 2 displays the results. It is encouraging that the model fits the U.S. wealth distribution reasonably well, particularly the right tail. It thus provides a reliable platform for evaluating the distributional implications of robustness over the business cycle.

Table 2: Stationary wealth distribution

	Data	Model
$P(a<0)$	0.100	0.128
$[0,50)$	0.018	0.036
$[50,90)$	0.251	0.206
$[90,99)$	0.382	0.434
$[99,100]$	0.350	0.324
Gini	0.860	0.828

Notes: The source of the data is the Survey of Consumer Finances.

4.2 Computation

To solve the competitive equilibrium with volatility shocks, we employ the approximation method developed by Krusell and Smith (1997) and specifically the continuous-time version of Fernández-Villaverde et al. (2019). The method assumes that households are boundedly rational in the sense that they only use partial information in the distribution to predict the law of motion for the state variables. More precisely, the paper postulates that the aggregate capital stock K_t is a sufficient statistic to represent the distribution function G_t, with the following perceived law of motion (PLM) of aggregate capital and risk-free rate

$$\begin{aligned} dK_t &= p(K_t, \vartheta_t)dt \\ r_t &= r(K_t, \vartheta_t), \end{aligned} \tag{4.1}$$

where $p(\cdot)$ and $r(\cdot)$ are two forecasting functions specified as

$$\begin{aligned} p(K_t, \vartheta_t) &= \beta_1 + \beta_2\vartheta_t + \beta_3 \ln K_t + \beta_4\vartheta_t \ln K_t \\ r(K_t, \vartheta_t) &= \beta_5 + \beta_6\vartheta_t + \beta_7 \ln K_t + \beta_8\vartheta_t \ln K_t, \end{aligned} \tag{4.2}$$

for some unknown parameters $\beta = (\beta_1, \cdots, \beta_8)$. Based on the postulated PLM (4.1), problem (2.14) can be characterized by the following approximated HJB equation:

$$\begin{aligned} \rho v(a, z_j, K, \vartheta) = \max_{c,k} \min_h \frac{c^{1-\gamma}}{1-\gamma} + \frac{1}{2\varepsilon} h^2 + s(a, z_j, K, \vartheta) \frac{\partial v}{\partial a} + \lambda_j \left(v(a, z_{-j}, K, \vartheta) - v(a, z_j, K, \vartheta) \right) \\ + \frac{\vartheta k^2}{2} \frac{\partial^2 v}{\partial a^2} + p(K, \vartheta) \frac{\partial v}{\partial K} + \theta(\bar{\vartheta} - \vartheta) \frac{\partial v}{\partial \vartheta} + \frac{\vartheta \nu^2}{2} \frac{\partial^2 v}{\partial \vartheta^2}, \end{aligned} \tag{4.3}$$

where the robust saving function $s(a, z_j, K, \vartheta)$ is such that

$$s(a, z_j, K, \vartheta) = w(K, \vartheta) z_j + r(K, \vartheta) a + \left(R(K, \vartheta) - r(K, \vartheta) + \sqrt{\vartheta} h \right) k - c, \tag{4.4}$$

with $w(K, \vartheta)$ and $R(K, \vartheta)$ denoting wage and expected capital return given in (3.1).

We solve the HJB equation (4.3) and simulate the economy over a long period of time using an upward finite difference scheme advocated by Achdou et al. (2022). The resulting model generated moments are compared to those perceived by households. If they are close enough, then one obtains a good approximation of the equilibrium. Otherwise, one could try different functional forms of the forecasting functions p and r, or include additional moments of the distribution G. Technical details of the numerical algorithm are presented in the Appendix B.

5 Quantitative results

This section deploys the parameterized model to investigate the role of model uncertainty over the business cycle, from both aggregate and distributional perspectives.

5.1 Aggregate effects of a risk shock

We first find the deterministic steady state (DSS) model version in which all the shocks are kept at their mean levels (mostly zero). Figure 2 exhibits the aggregate dynamics, measured by percentage deviations of involved variables from the DSS, following a sudden escalation in volatility (green solid line). Heightened risk in the entrepreneurial activity depresses the demand for the risky capital, resulting in a deep decline in capital stock, output, and wage, and a sharp increase in the expected capital return. As households accumulate more bonds out of precautionary motive, the risk-free interest rate drops, yielding a spike in the equity premium. When the volatility shock hits, consumption rises on impact before subsequently falling back below its steady-state level.[10] The initial jump of consumption is a well-known feature of a business cycle model with pure volatility shocks as shown in Bloom et al. (2018). In the current model, the result stems largely from a substitution effect because the negative risk shock makes it more attractive for households to consume today rather than tomorrow as lower interest rate make savings less attractive.

Figure 2: Effects of risk shock on aggregate variables

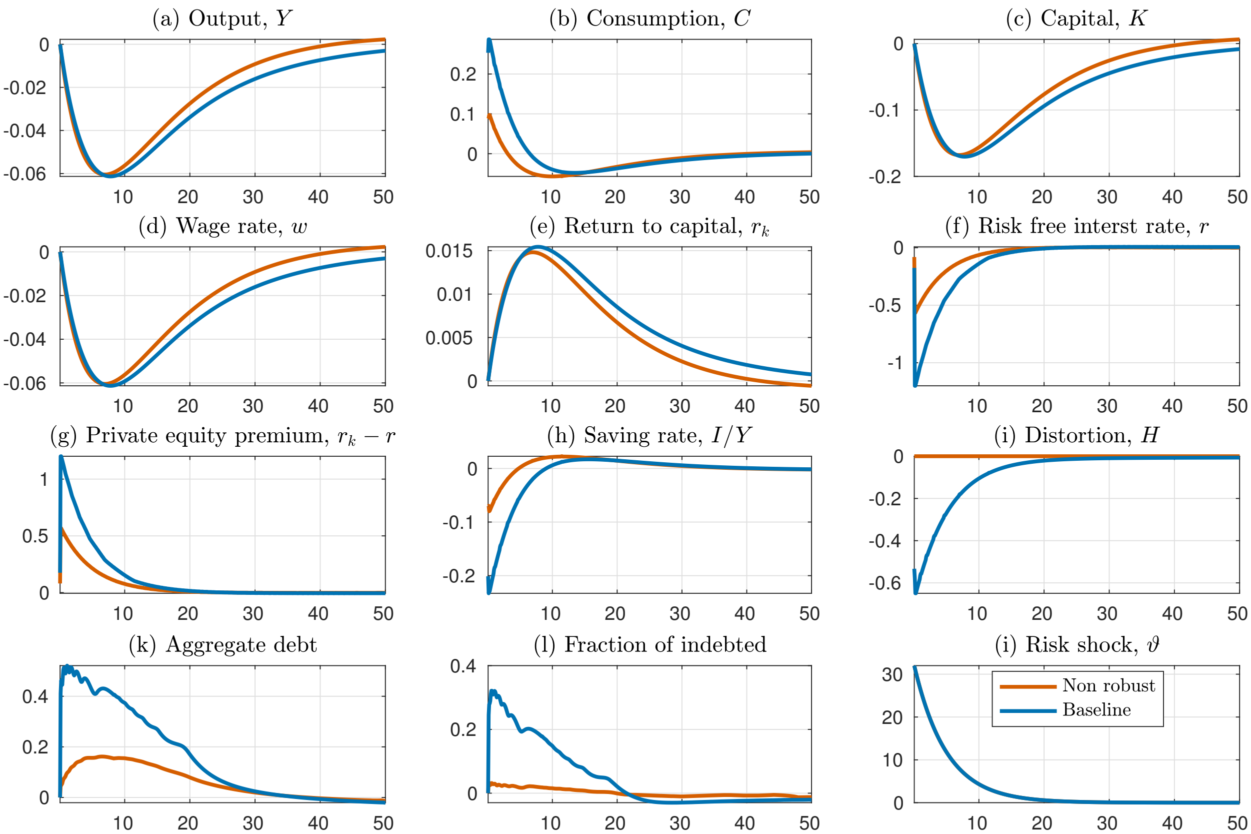

Notes: Panel (k) reports aggregate debt defined as $\frac{B}{K} = \frac{\int_{b<=0} bdG(a,z)}{K}$ and panel (l) shows the fraction of indebted households given by $\int_{b<=0} dG(a,z)$

We next examine the role of robustness in the economic repercussions driven by volatility shocks. For comparison, we display in Figure 2 the ensuing impulse responses in a counterfactual economy that is identical to the benchmark except for robustness (red dashed line). There are two main takeaways from the figure. First of all, the drop in the risk-free interest rate on impact is far and away larger in the benchmark economy. After the elevation in aggregate volatility, the fear of misspecifying the capital return process

[10]The literature has proposed multiple ways to resolving this anomaly by, for example, introducing additional saving vehicles in Fernández-Villaverde et al. (2011) or modeling precautionary savings from households in the wake of a volatility shock in Basu and Bundick (2017). Including these modifications would add little additional insight but increase the computational burden considerably. We have thus abstracted from these expansions in the paper.

intensifies immediately (larger σ in (3.22)). Households become more pessimistic right away and speed up their portfolio rebalancing toward the safe asset, making the decline in the risk-free rate much steeper. Consequently, due to the slow adjustments of capital stock and thus the expected capital return by (3.1), the initial jump in the equity premium is also more pronounced in the benchmark economy. Accelerated divestment in the risky capital, as evidenced in the more suppressed investment rate, helps magnify the early rise in consumption. Decreases in output and wage are, however, similar on impact in the two economies as they move in lock step with capital in light of Proposition 1.

The second finding is that model uncertainty notably slows the economy's recovery from the depth of the recession. As the volatility shock subsides, entrepreneurs are starting to take advantage of low labor and borrowing costs and build up their capital stock. However, the incentive is weaker in the benchmark economy, because the wealth losses experienced in the early stage of the downturn encourage nature to keep distorting the risky return model (2.12) aggressively until households sufficiently restore their wealth (smaller a in (3.22)). This, in turn, weighs on their subjective evaluation of the prospect capital return, and slows down their investment. Therefore, while the depth of recessions is comparable in the two economies, the recovery of capital and output is more sluggish in the benchmark.

5.2 Distributional effects of a risk shock

In this subsection, we explore the distributional implications of robustness for the propagation of volatility shocks. Figure 3 depicts the impulse responses of wealth, consumption, holdings of capital and bond, and model distortion to the same volatility shock in Figure 2 for three individual wealth groups.[11] To distinguish the role of robustness, we similarly report the model-implied dynamics in both benchmark (blue solid line) and nonrobust (red solid line) economies.

As shown, there is a vast heterogeneity in the responses of consumption and portfolio variables to the volatility shock across the wealth distribution. For households whose wealth ranks over the top 10 percent in the population, a spike in the aggregate volatility propels a wealth reallocation from the risky capital to the riskless bond. This is because these households hold majority of their wealth in the private capital, and a negative risk shock begets a flight-to-safety. The rebalanced portfolio, however, features a lower overall return, leading to a subsequent decline in wealth and consumption from their steady-state levels. When households are uncertain about the underlying capital return process,

[11] In the figure, a group-specific variable refers to the average of the variable of households whose wealth fall into that group.

Figure 3: Effects of risk shock on group-specific average

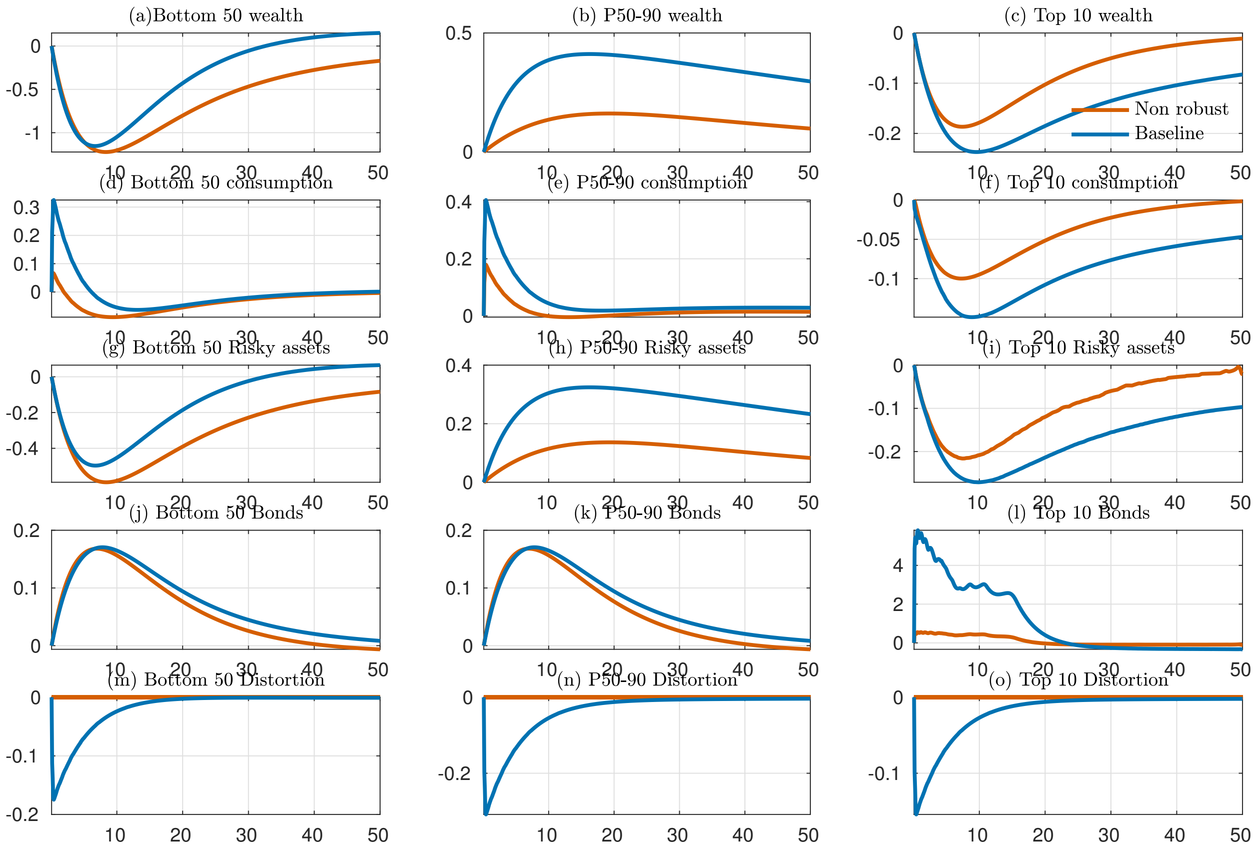

an elevated volatility only aggravates their concerns about possibly misspecifying the return model (2.12) with a large jump in distortion from nature. As such, these households accelerate reallocating their wealth from the private capital to the bond market, yielding a more precipitous decrease in wealth and consumption. In essence, model uncertainty considerably strengthens the precautionary saving motive of wealth-rich households, and it helps supercharge their portfolio reallocation activity. Since they are the primary holders of the capital stock, this intensified reallocation manifests itself in a more pronounced interest-rate slump in the benchmark economy as seen in Figure 2.

By contrast, for households owning intermediate levels of wealth, i.e., those within the p50-90 wealth bracket, the negative volatility shock creates an opportunity for growing their wealth. The combination of lower risk-free rate and higher excess capital return, engineered by the portfolio rebalancing of their richer counterparts, encourages these households to tap the bond market and use the proceeds to invest in the capital.[12] The readjusted portfolio provides a higher average return and helps expand their wealth and

[12]We invite the reader to interpret the initial upward movement in panel (k) and (j) as an accumulation of debt since each panel measures the percentage deviation from the steady-state level of bonds held by respective group, both of which are negative (or simply debt) in the numerical simulation.

consumption after the volatility shock, a stark contrast to their respective dynamics for households in the top 10 percent wealth group. More interestingly, we find that model uncertainty tends to reinforce this portfolio adjustment as evidenced in a much stronger growth in the holding of the risky capital. This is because although elevated volatility increases the pessimism about the capital return, its negative effect on capital investment is outweighed by the associated general equilibrium benefits due to the steeper decline in the interest rate and rise in the expected capital return than in the scenario absent robustness.

Meanwhile, decreasing wage and thus labor income after the volatility shock makes it more difficult for households in the bottom 50 percent wealth group to prop up their consumption than the rest. For them human wealth constitutes a more important funding source than financial wealth, whose accumulation is also limited by the borrowing constraint. In response, these wealth-poor households liquidate their capital and borrow in the bond market at an interest rate cheaper than before. However, as model uncertainty has triggered a much larger decline in the rate, they don't have to sell their capital as much as they would do in the counterfactual economy without robustness. This accounts for the observed less severe drop in capital and wealth, and stronger pick-up in consumption.

The above analysis demonstrates that in comparison to its aggregate implications, robustness acts as a powerful distributional amplifier of volatility shocks by significantly magnifying the fluctuations of consumption and portfolio variables across the wealth spectrum. It crystallizes the importance of incorporating household heterogeneity for assessing the business-cycle implications of model uncertainty. But it remains unclear how and to which extent it would reshape the evolution of economic distributions. To gain insight into this point, Figures 4 plot in order the distributional dynamics of wealth and consumption driven by the same negative volatility shock. Each figure displays the changes in dispersion and skewness of the corresponding distribution, where the second and third moments are inferred from the 10th, 50th and 90th percentiles of the distribution. These quantile-based statistics are robust to outliers and also easy to interpret. We use the ratio between the 90th and 10th percentiles, $P9010$ in Panel (b), to measure the overall dispersion, and similarly, the ratios between the 50th and 10th percentiles, $P5010$ in Panel (c), and between the 90th and 50th percentiles, $P9050$ in Panel (d) to represent dispersion in the left and right tails, respectively. Our measure of skewness in Panel (a) is the Kelley skewness defined as $KSK = \frac{(P90-P50)-(P50-P10)}{P90-P10} = \frac{P9050*P5010-2*P5010+1}{P9050*P5010-1}$. A positive value of the skewness indicates that the right tail accounts for more than one half of the total dispersion or the distribution is rightly skewed, and vice versa for a negative value.

Figure 4: Effects of risk shock on wealth and consumption inequality

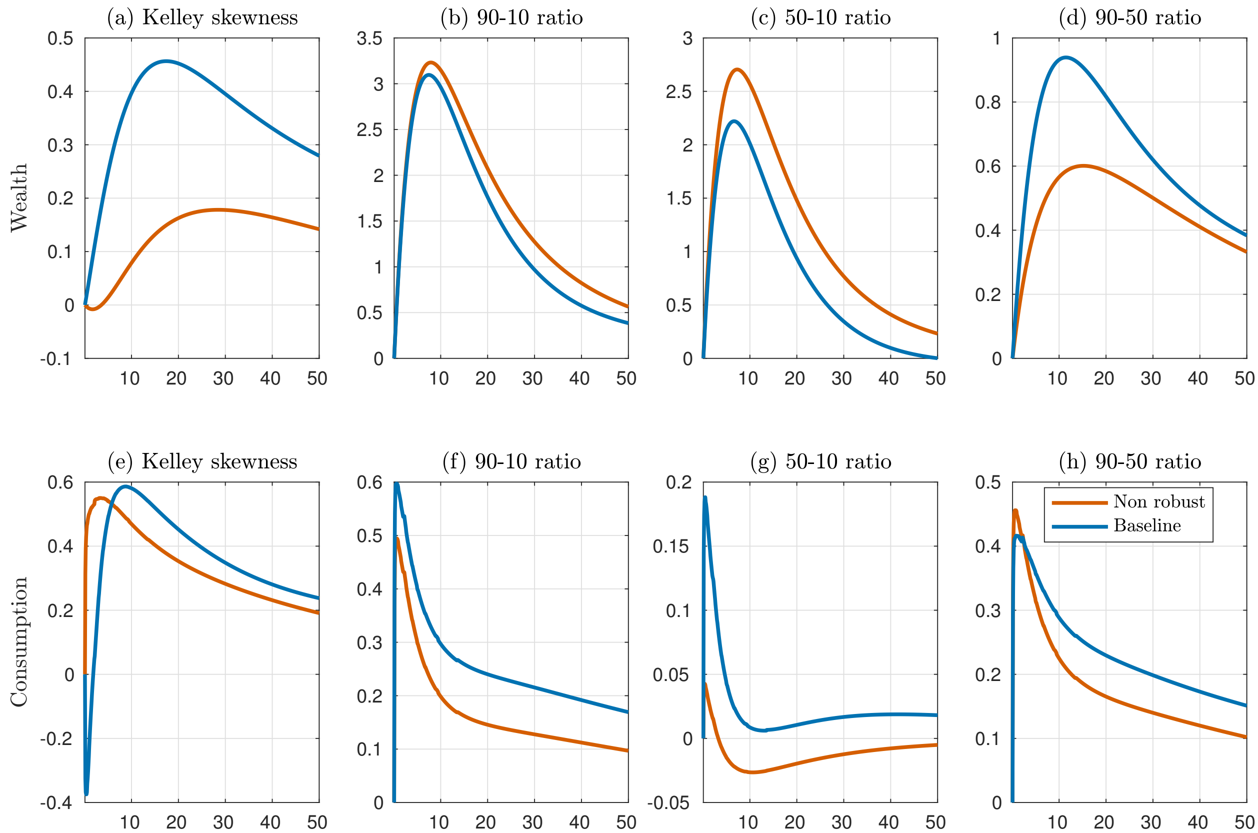

Notes: We transform the joint distribution of wealth and income, $g(a,z)$, into a joint distribution of consumption and income, $f(c,z)$, as follows: $f(c,z) = \frac{g(c^{-1}(a,z),z)}{|c_a(a,z)|}$, where $(c^{-1}(a,z),z)$ is the inverse of the vector $(c(a,z),z)$ and $c_a(a,z)$ is the slope of consumption with respect to wealth. The Kelley measure is defined as : $KSK = \frac{(P90-P50)-(P50-P10)}{P90-P10}$. A negative value indicates that the left-tail contribution to the overall dispersion is larger than that of the right tail.

The first row of figure 4 shows that heightened investment risk widens the wealth dispersion in both tails and thus the total dispersion. The skewness also picks up after the shock, suggesting that the rise in dispersion is more acute in the right tail. It is noteworthy that robustness exerts strong but opposite impacts on dispersion in the two tails: it markedly enlarges dispersion in the right tail but limits that in the left. This asymmetric change is in line with the observed adjustments of the risky capital by the first two wealth groups in Figure 3, as wealth dispersion moves largely in tandem with the capital in the model.[13] Consequently, despite its relatively muted effect on the overall dispersion, robustness considerably skews the distribution further rightward as seen in the steeper elevation in the Kelley skewness.

There are, however, some notable differences in the way consumption distribution re-

[13]The current measures of dispersion and skewness are constructed without considering the top and bottom 10 percent of the distribution. By design, it ignores the distributional effects of behavioral changes from households in the top 10 percent wealth group. Using wider symmetric percentiles, such as the 95th and 5th percentiles, is found to have limited impacts on the results.

acts to robustness relative to that of wealth. The second row of figure 4 shows that model uncertainty multiplies instead of dampens the increase in total dispersion of consumption over the risk-driven downturn. The divergence is propelled by a much stronger uptick in the left-tail dispersion in the benchmark economy, especially at the onset of the shock. This mainly stems from a well-known substitution effect as the steeper decline in risk-free interest rate in the benchmark prompts a larger jump in consumption for households near the right end of the bottom 50 group. In consequence, model uncertainty skews the consumption distribution leftward on impact before reversing the course subsequently.

5.3 The role of household heterogeneity

To help gain additional insights into the role of incomplete asset markets, we compare in this section models with different degrees of heterogeneity. More precisely, we compare our baseline model with a model economy were all the parameters are kept to their baseline values except for the volatility of the idiosyncratic investment risk. In this alternative economy, we decrease the value of volatility of the idiosyncratic investment risk by 28 percent going from $\sigma = 0.125$ to $\sigma = 0.09$. Figure 5 below and figure 7-9 in the appendix compares our baseline economy to such an economy with low degree of investment risk. The alternative economy behaves similar to our baseline model but induces a smaller response to volatility shocks. The peak in consumption response on impact is dampened by a factor of about 30 in a robust economy with low investment risk (dashed blue line) relative to the baseline. Intuitively, the lower the degree of heterogeneity, the easier it is for household to smooth consumption by reducing their self-insurance needs and investing more in the private firm.

Figure 5: Effects of risk shock on aggregate variables by investment risk level

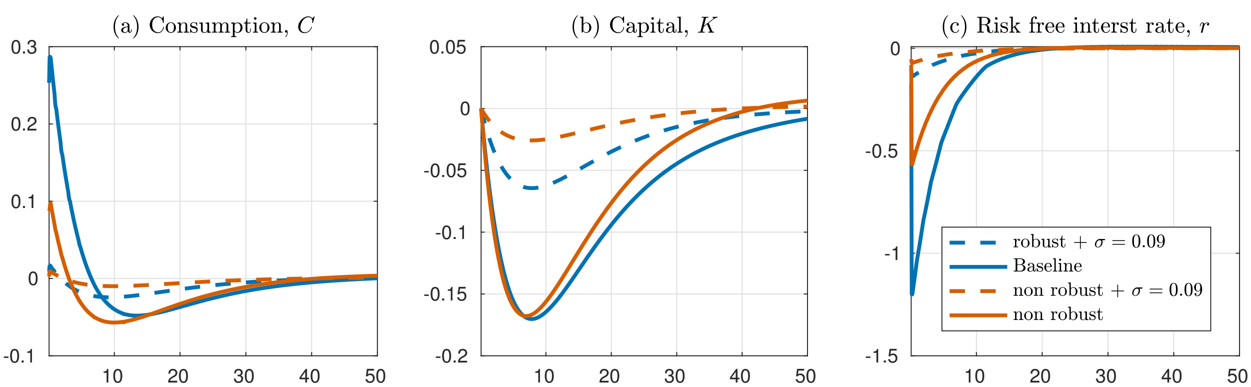

Notes:

5.4 Extension with both TFP and risk shocks

In this section, we examine the robustness of the insights derived above by considering an additional aggregate TFP shock. This can also be interpreted that recessions, such as the Great Recession, are typically periods of both first- and second-moment shocks. The extended model is only a minimal departure from the benchmark, where entrepreneurs operate production using the following technology:

$$y_t = e^{Z_t} F(k_t, l_t) = e^{Z_t} k_t^{\alpha} l_t^{1-\alpha}, \tag{5.1}$$

with Z_t being the logarithm of aggregate productivity. For computational tractability, we assume Z_t follows a two-state Poisson process and takes values in $\{Z_1, Z_2\}$ with $Z_1 < Z_2$. The process jumps from state 1 to state 2 with intensity ψ_1 and from state 2 to state 1 with intensity ψ_2.

The stochastic process of aggregate productivity is calibrated under the interpretation that the economy enters into recession and expansion in state Z_1 and Z_2, respectively. The jump intensities ψ_1 and ψ_2 are chosen to match the frequency of U.S. recessions $\frac{\psi_2}{\psi_1+\psi_2} = \frac{10}{10+60}$ and the average length of a recession $\frac{1}{\psi_1} = 10/12$ years using the NBER-dated recessions. We estimate the ratio of productivity $\frac{e^{Z_1}}{e^{Z_2}} = 0.9648$, from the post-World War II US economy log of TFP series of Fernald (2014). The combination of the productivity ratio together with the fact the stationary mean log productivity is normalized to be zero, i.e $\frac{\psi_2}{\psi_1+\psi_2} Z_1 + \frac{\psi_1}{\psi_1+\psi_2} Z_2 = 0$, pin down the values of Z_1 at -0.0307 and Z_2 at 0.0051.

Table 3: Business cycle moments

	Data	Baseline	Nonrobust
$\sigma(Y)$	0.015	0.009	0.009
$\sigma(C)/\sigma(Y)$	0.550	0.446	0.403
$\sigma(I)/\sigma(Y)$	4.137	3.416	3.381
$corr(C, Y)$	0.835	0.929	0.958
$corr(I, Y)$	0.930	0.981	0.991
$corr(Y_t, Y_{t-1})$	0.874	0.723	0.723

Notes: All aggregate variables are log-transformed. Empirical moments are computed based on quarterly aggregate data from 1984Q1 to 2019Q4 HP filtered. We simulate the model for a long sample and HP filtered the generated data while accounting for a burn-in. We then compute the model equivalent of each empirical moment using these data.

As a validation, we compare the dynamics of economic variables implied by the extended model and the data. We simulate our model with a sequence of aggregate risk and TFP shocks, and use the HP-filtered series to compute business cycle moments. Results are reported in Table 3. It suggests that our model successfully reproduces the relative volatilities and cyclical behavior of consumption, investment, and capital stock observed in data even though we did not directly target those moments in our calibration. Relative to the non robust economy counterpart, all aggregates macroeconomics variable are more volatile in our baseline robust economy. Consumption volatility is about 11 per cent higher. As discussed in previous sections, household consumption-portfolio choice problem under Knightian uncertainty driving the returns to private capital returns combined with borrowing constraint explain the business cycle fluctuations amplification mechanism present in the baseline economy.

In figure 6, we plot the model impulse response to a onetime positive two standard deviation increase in risk shocks combined with a productivity sequence where aggregate TFP is kept at state $Z = Z_1$ for 10 months before returning to its stationary mean. Consumption, capital and interest rate all fall on impact and recover thereafter. The addition of TFP shocks thus corrects the consumption impulse response anomaly documented earlier. As a results, these dynamics adjustment to shocks create plausible recessions driven by model uncertainty.

Figure 6: Effects of risk and TFP shocks on aggregate variables

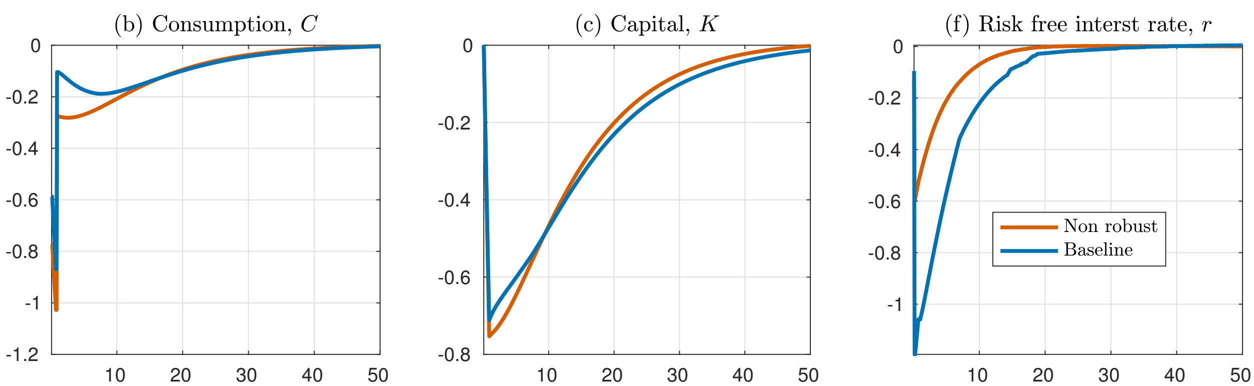

Notes:

6 Conclusion

This paper examines the implications of model uncertainty for wealth distribution and business cycles in a tractable continuous-time general equilibrium model. We find that the size of the model distortion chosen by nature varies nonmonotonically with household wealth. Robustness generates a larger concentration of wealth due to two factors. It increases the speed at which the wealth of unlucky households hits the borrowing constraint. It also leads richer households to invest a disproportionally larger share of wealth in the higher yielding asset. Our analysis shows that robustness significantly prolongs the recession driven by an investment risk shock, and magnifies the associated fluctuations of consumption and portfolio variables across the wealth spectrum.

To illustrate the distributional effects of robustness, the model is deliberately kept simple. The mechanism proposed in the paper, however, opens the door to a proper quantitative analysis. For example, an emerging body of evidence highlights that in order to understand the aggregate economic activities during the Great Recession, it is crucial for a model to capture the large fraction of poor households.[14] Model uncertainty provides a useful channel through which a substantial share of the population become wealth poor.

References

Achdou, Yves, Jiequn Han, Jean-Michel Lasry, Pierre-Louis Lions, and Benjamin Moll, "Income and wealth distribution in macroeconomics: A continuous-time approach," *Review of Economic Studies*, 2022, *89* (1), 45–86.

Aiyagari, S Rao, "Uninsured idiosyncratic risk and aggregate saving," *Quarterly Journal of Economics*, 1994, *109* (3), 659–684.

Anderson, Evan W, Lars Peter Hansen, and Thomas J Sargent, "A quartet of semigroups for model specification, robustness, prices of risk, and model detection," *Journal of the European Economic Association*, 2003, *1* (1), 68–123.

Angeletos, George-Marios, "Uninsured idiosyncratic investment risk and aggregate saving," *Review of Economic Dynamics*, 2007, *10* (1), 1–30.

Backus, David, Axelle Ferriere, and Stanley Zin, "Risk and ambiguity in models of business cycles," *Journal of Monetary Economics*, 2015, *69*, 42–63.

Basu, Susanto and Brent Bundick, "Uncertainty shocks in a model of effective demand," *Econometrica*, 2017, *85* (3), 937–958.

Benhabib, Jess, Alberto Bisin, and Shenghao Zhu, "The wealth distribution in Bewley economies with capital income risk," *Journal of Economic Theory*, 2015, *159*, 489–515.

_ , _ , and _ , "The distribution of wealth in the Blanchard–Yaari model," *Macroeconomic Dynamics*, 2016, *20* (2), 466–481.

[14]Existing proposals include heterogeneous preferences and rich earning processes, e.g., Krueger et al. (2016) and De Nardi and Fella (2017).

Bewley, Truman, "Stationary monetary equilibrium with a continuum of independently fluctuating consumers," *Contributions to mathematical economics in honor of Gérard Debreu*, 1986, *79*.

Bidder, Rhys M and Matthew E Smith, "Robust animal spirits," *Journal of Monetary Economics*, 2012, *59* (8), 738–750.

Blanchard, Olivier J and Jordi Galí, "Labor markets and monetary policy: A new Keynesian model with unemployment," *American Economic Journal: Macroeconomics*, 2010, *2* (2), 1–30.

Bloom, Nicholas, Max Floetotto, Nir Jaimovich, Itay Saporta-Eksten, and Stephen J Terry, "Really uncertain business cycles," *Econometrica*, 2018, *86* (3), 1031–1065.

Brenner, Menachem and Yehuda Izhakian, "Asset pricing and ambiguity: Empirical evidence," *Journal of Financial Economics*, 2018, *130* (3), 503–531.

Cao, Dan and Wenlan Luo, "Persistent heterogeneous returns and top end wealth inequality," *Review of Economic Dynamics*, 2017, *26*, 301–326.

Dimmock, Stephen G, Roy Kouwenberg, Olivia S Mitchell, and Kim Peijnenburg, "Ambiguity aversion and household portfolio choice puzzles: Empirical evidence," *Journal of Financial Economics*, 2016, *119* (3), 559–577.

Fernald, John, "A quarterly, utilization-adjusted series on total factor productivity," in "in" Federal Reserve Bank of San Francisco 2014.

Fernández-Villaverde, Jesús, Pablo Guerrón-Quintana, Juan F Rubio-Ramírez, and Martin Uribe, "Risk matters: The real effects of volatility shocks," *American Economic Review*, 2011, *101* (6), 2530–2561.

_ , Samuel Hurtado, and Galo Nuno, "Financial frictions and the wealth distribution," Technical Report, National Bureau of Economic Research 2019.

Gabaix, Xavier, Jean-Michel Lasry, Pierre-Louis Lions, and Benjamin Moll, "The dynamics of inequality," *Econometrica*, 2016, *84* (6), 2071–2111.

Gilboa, Itzhak and David Schmeidler, "Maxmin expected utility with non-unique prior," *Journal of Mathematical Economics*, 1989, *18* (2), 141–153.

Hall, Robert E. and Paul R. Milgrom, "The limited influence of unemployment on the wage bargain," *American Economic Review*, 2008, *98* (4), 1653–1674.

Hansen, Lars Peter and Thomas Sargent, *Robustness*, Princeton University Press, 2008.

__ **, Thomas J. Sargent, Gauhar Turmuhambetova, and Noah Williams**, "Robust control and model misspecification," *Journal of Economic Theory*, May 2006, *128* (1), 45–90.

Huggett, Mark, "The risk-free rate in heterogeneous-agent incomplete-insurance economies," *Journal of Economic Dynamics and Control*, 1993, *17* (5-6), 953–969.

Kaplan, Greg, Benjamin Moll, and Giovanni L. Violante, "Monetary policy according to HANK," *American Economic Review*, March 2018, *108* (3), 697–743.

Kasa, Kenneth and Xiaowen Lei, "Risk, uncertainty, and the dynamics of inequality," *Journal of Monetary Economics*, 2018, *94*, 60–78.

Krueger, Dirk, Kurt Mitman, and Fabrizio Perri, "Macroeconomics and household heterogeneity," in "Handbook of Macroeconomics," Vol. 2, Elsevier, 2016, pp. 843–921.

Krusell, Per and Anthony A Smith, "Income and wealth heterogeneity, portfolio choice, and equilibrium asset returns," *Macroeconomic Dynamics*, 1997, *1* (2), 387–422.

Luo, Yulei, Jun Nie, and Eric R Young, "Ambiguity, Low Risk-Free Rates and Consumption Inequality," *Economic Journal*, 2020, *130* (632), 2649–2679.

Maccheroni, Fabio, Massimo Marinacci, and Aldo Rustichini, "Ambiguity aversion, robustness, and the variational representation of preferences," *Econometrica*, 2006, *74* (6), 1447–1498.

Maenhout, Pascal J, "Robust portfolio rules and asset pricing," *Review of Financial Studies*, 2004, *17* (4), 951–983.

Moskowitz, Tobias J and Annette Vissing-Jørgensen, "The returns to entrepreneurial investment: A private equity premium puzzle?," *American Economic Review*, 2002, *92* (4), 745–778.

Nardi, Mariacristina De and Giulio Fella, "Saving and wealth inequality," *Review of Economic Dynamics*, 2017, *26*, 280–300.

Nuno, Galo and Benjamin Moll, "Social optima in economies with heterogeneous agents," *Review of Economic Dynamics*, 2018, *28*, 150–180.

Quadrini, Vincenzo and José-Víctor Ríos-Rull, "Inequality in macroeconomics," in "Handbook of Income Distribution," Vol. 2, Elsevier, 2015, pp. 1229–1302.

Strzalecki, Tomasz, "Axiomatic foundations of multiplier preferences," *Econometrica*, 2011, *79* (1), 47–73.

Tella, Sebastian Di and Robert Hall, "Risk premium shocks can create inefficient recessions," *Review of Economic Studies*, 2022, *89* (3), 1335–1369.

Toda, Alexis Akira and Kieran James Walsh, "The equity premium and the one percent," *Review of Financial Studies*, 2020, *33* (8), 3583–3623.

A Proofs

A.1 Proof of Proposition 1

Given the installment of capital and the observation of shocks, an entrepreneur hires workers to maximize its profit:

$$\varpi(k) = \max_{l} k^{\alpha} l^{1-\alpha} - wl - \delta k. \tag{A.1}$$

It is straightforward to verify that the optimal employment and profit are

$$l(k) = \left(\frac{w}{1-\alpha}\right)^{-\frac{1}{\alpha}} k,\ \varpi(k) = \left(\left(\frac{w}{1-\alpha}\right)^{-\frac{1-\alpha}{\alpha}} - w\left(\frac{w}{1-\alpha}\right)^{-\frac{1}{\alpha}} - \delta\right) k, \tag{A.2}$$

both of which are linear in k. Integrating $l(k)$ with respect to the density g_t and using the labor market clearing condition (2.17) yield the equilibrium wage

$$w_t = w(K_t, \vartheta_t) = (1-\alpha) K_t^{\alpha}, \tag{A.3}$$

and the associated profit

$$\varpi(k_t) = R(K_t, \vartheta_t) k_t,\ R(K, \vartheta) = \alpha K^{\alpha-1} - \delta. \tag{A.4}$$

Combining (2.4) and (A.4) gives the equilibrium dynamics of the capital income

$$d\varpi_t = R(K_t, \vartheta_t) k_t dt + \sqrt{\vartheta_t} k_t dW_t, \tag{A.5}$$

and consequently by (2.7) that of the capital return

$$d\tilde{R}_t = R_t dt + \sqrt{\vartheta_t} dW_t,\ R_t = R(K_t). \tag{A.6}$$

By (A.2) and (A.3), aggregate output equals

$$Y_t = \sum_{j=1}^{2} \int y g_t(a, z_j) = \sum_{j=1}^{2} \int \left(\frac{w(K_t, \vartheta_t)}{1-\alpha}\right)^{-\frac{1-\alpha}{\alpha}} k g_t(a, z_j) = K_t^{\alpha}. \tag{A.7}$$

Aggregating individual budget constraints (2.9) and employing the market clearing conditions (2.16) and (2.17) yield the following dynamics of the aggregate capital

$$\begin{aligned} dK_t &= \sum_{j=1}^{2} \int \left(w_t z_j + r_t a + \hat{\pi}_t k - c \right) g_t(a, z_j) + \sum_{j=1}^{2} \sqrt{\vartheta_t} \int k g_t(a, z_j) dW_t \\ &= \left(w_t + R_t K_t - C_t \right) dt = \left(K_t^{\alpha} - \delta K_t - C_t \right) dt, \end{aligned} \tag{A.8}$$

where the term associated with $\sum_{j=1}^{2} \int k g_t(a, z_j) dW_t$ disappears because idiosyncratic shocks wash away in aggregation.

A.2 Proof of Proposition 2

To prove Part 1 of the proposition, we first show that $s_1(\underline{a}) = 0$. The FOCs of problem (3.3) associated with c, k, h are, respectively,

$$u'\left(c_j(a)\right) = v_j'(a) \tag{A.9}$$

$$v_j'(a)\left(R + \sigma h_j(a) - r\right) + v_j''(a)\,\sigma^2 k_j(a) = 0 \tag{A.10}$$

$$h_j(a) + \varepsilon\sigma v_j'(a)\,k_j(a) = 0. \tag{A.11}$$

Since $0 \le k_j(a) \le a - \underline{a}$, it follows that $\lim_{a \to \underline{a}} k_j(a) = 0$, and by (A.11) $\lim_{a \to \underline{a}} h_j(a) = 0$, where the last equality uses the fact that $v_j'(\underline{a}) = \lim_{a \to \underline{a}} u'\left(c_j(a)\right) < \infty$. Evaluating the Euler equation of problem (3.3) at $a = \underline{a}$ with (A.9) and $k(\underline{a}) = 0$ yields

$$\rho - r = \frac{u''(c_1(\underline{a}))}{u'(c_1(\underline{a}))} c_1'(\underline{a}) s_1'(\underline{a}) + \lambda_1 \left(\frac{u'(c_2(\underline{a}))}{u'(c_1(\underline{a}))} - 1 \right). \tag{A.12}$$

Given $u' > 0$, $u'' < 0$, $c_1' \ge 0$ and $c_2(a) \ge c_1(a)$, equation (A.12) implies $s_1(\underline{a}) \le 0$. Observing the borrowing constraint $a \ge \underline{a}$ requires $s_1(\underline{a}) = 0$, and consequently

$$c_1(\underline{a}) = \lim_{a \to \underline{a}} w z_1 + r a + (R + \sigma h_1(a) - r) k_1(a) - s_1(a) = w z_1 + r\underline{a} > 0.$$

As a matter of fact, $s_1(\underline{a}) < 0$ in a neighborhood of the borrowing constraint. To see this more precisely, combining (2.8), (A.10) and (A.11) yields

$$k_j(a) = \min\left\{ \frac{R - r}{\sigma^2} \frac{v_j'(a)}{\varepsilon v_j'^2 - v_j''(a)}, a + \phi \right\}. \tag{A.13}$$

As a consequence, we have

$$0=\lim_{a\to\underline{a}}k_1(a)=\lim_{a\to\underline{a}}-\frac{v_1'(a)}{v_1''(a)}\frac{R+\sigma h_1(a)-r}{\sigma^2}=-\frac{u'(c_1(\underline{a}))}{u''(c_1(\underline{a}))\,c_1'(\underline{a})}\frac{R-r}{\sigma^2},$$

meaning that $c_1'(\underline{a})=\infty$. Because $0\leq k_1(a)\leq a-\underline{a}$ and $k_1(\underline{a})=0$, it holds that

$$k_1'(\underline{a})=\lim_{a\to\underline{a}}\frac{k_1(a)-k_1(\underline{a})}{a-\underline{a}}=\lim_{a\to\underline{a}}\frac{k_1(a)}{a-\underline{a}}\leq\lim_{a\to\underline{a}}\frac{a-\underline{a}}{a-\underline{a}}=1,$$

i.e., $k_1'(\underline{a})$ is bounded. Differentiating (A.11) with respect to a yields

$$h_j'(a)=-\varepsilon\sigma\left(v_j''(a)\,k_j(a)+v_j'(a)\,k_j'(a)\right). \tag{A.14}$$

As a result, we have

$$\begin{aligned}\lim_{a\to\underline{a}}s_1'(a) &= \lim_{a\to\underline{a}}r+k_1'(a)\,(R+\sigma h_1(a)-r)+k_1(a)\,\sigma h_1'(a)-c_1'(a) \qquad (A.15)\\ &= \lim_{a\to\underline{a}}r+k_1'(a)\,(R+\sigma h_1(a)-r)-\varepsilon\sigma^2 k_1(a)\begin{pmatrix}v_1''(a)\,k_1(a)+\\ v_1'(a)\,k_1'(a)\end{pmatrix}-c_1'(a)\\ &= -\infty,\end{aligned}$$

where the last equality stems from the fact that $\lim_{a\to\underline{a}}k_1(a)=\lim_{a\to\underline{a}}h_1(a)=0$, and the two limits $\lim_{a\to\underline{a}}k_1'(a)$ and $\lim_{a\to\underline{a}}v_1''(a)\,k_1(a)=-\lim_{a\to\underline{a}}v_1'(a)\,\frac{R+\sigma h_1(a)-r}{\sigma^2}$ are bounded. Since $s_1(\underline{a})=0$, it holds that there exists $\delta>0$ such that $s_1(a)<0$ for $a\in(\underline{a},\underline{a}+\delta)$.

We now proceed to derive the approximate analytical solution of $s_1(a)$ near the borrowing constraint. By definition,

$$\begin{aligned}\lim_{a\to\underline{a}}\left(s_1'(a)+c_1'(a)\right)s_1(a) &= \lim_{a\to\underline{a}}\left(r+(R-r+\sigma h_1(a))\,k_1'(a)+k_1(a)\,\sigma h_1'(a)\right)s_1(a)\\ &= \lim_{a\to\underline{a}}\begin{pmatrix}r+(R-r+\sigma h_1(a))\,k_1'(a)\\ -\varepsilon\sigma^2 k_1(a)\,(v_1''(a)\,k_1(a)+v_1'(a)\,k_1'(a))\end{pmatrix}s_1(a)=0,\end{aligned}$$

which implies that

$$\lim_{a\to\underline{a}}s_1'(a)\,s_1(a)=-\lim_{a\to\underline{a}}c_1'(a)\,s_1(a). \tag{A.16}$$

We next compute the limit on the right-hand side. The Euler equation of (3.3) is

$$
\begin{aligned}
\rho - r &= \frac{v_1''(a)}{v_1'(a)} s_1(a) + \frac{1}{2}\frac{v_1'''(a)}{v_1'(a)}\sigma^2 k_1^2(a) + \lambda_1\left(\frac{v_2'(a)}{v_1'(a)} - 1\right) \\
&= \frac{v_1''(a)}{v_1'(a)} s_1(a) + \frac{1}{2}\frac{v_1'''(a)}{v_1'(a)}\sigma^2\left(\frac{R-r}{\sigma^2}\frac{v_1'(a)}{\varepsilon v_1'(a)^2 - v_1''(a)}\right)^2 + \lambda_1\left(\frac{v_2'(a)}{v_1'(a)} - 1\right) \\
&\approx \frac{v_1''(a)}{v_1'(a)} s_1(a) + \frac{1}{2}\frac{v_1'''(a)}{v_1'(a)}\left(\frac{R-r}{\sigma}\right)^2\left(-\frac{v_1'(a)}{v_1''(a)} - \varepsilon\frac{v_1'(a)^3}{v_1''(a)^2}\right)^2 + \lambda_1\left(\frac{v_2'(a)}{v_1'(a)} - 1\right) \\
&\approx \frac{v_1''(a)\, s_1(a)}{v_1'(a)} + \frac{(R-r)^2}{2\sigma^2}\frac{v_1'''(a)\, v_1'(a)}{v_1''(a)^2}\left(1 + 2\varepsilon\frac{v_1'(a)^2}{v_1''(a)}\right) + \lambda_1\left(\frac{v_2'(a)}{v_1'(a)} - 1\right) \quad \text{(A.17)}
\end{aligned}
$$

By (A.9) and the functional form of u, we have

$$
\begin{aligned}
v_1'(a) &= u'(c_1(a)) = c_1(a)^{-\gamma} \\
v_1''(a) &= u''(c_1(a))\, c_1'(a) = -\gamma c_1(a)^{-\gamma-1} c_1'(a) \quad \text{(A.18)} \\
v_1'''(a) &= u'''(c_1(a))\, c_1'(a)^2 + u''(c_1(a))\, c_1''(a) = \gamma(\gamma+1)\, c_1(a)^{-\gamma-2} c_1'(a)^2 - \gamma c_1(a)^{-\gamma-1} c_1''(a).
\end{aligned}
$$

Substituting them into (A.17) and rearranging lead to

$$
\begin{aligned}
\rho - r &= -\gamma c_1(a)^{-1} c_1'(a)\, s_1(a) - \lambda_1 \gamma c_1(a)^{-1}(c_2(a) - c_1(a)) \quad \text{(A.19)} \\
&\quad + \frac{1}{2}\left(\frac{R-r}{\sigma}\right)^2\left(\frac{\gamma+1}{\gamma} - \frac{1}{\gamma} c_1(a)\frac{c_1''(a)}{c_1'(a)^2}\right)\left(1 - 2\varepsilon\frac{1}{\gamma}\frac{c_1(a)^{1-\gamma}}{c_1'(a)}\right).
\end{aligned}
$$

This together with (A.16) gives

$$
\lim_{a \to \underline{a}} s_1'(a)\, s_1(a) = \varsigma_1,
$$

where ς_1 is defined in (3.6). As a result, we have

$$
s_1(a)^2 \approx s_1(\underline{a})^2 + 2 s_1(\underline{a})\, s_1'(\underline{a})\,(a - \underline{a}) = 2\varsigma_1 (a - \underline{a}),
$$

and thus (3.5).

We next prove the second part of Proposition 2. The derivation of $\hat{\varsigma}_1$ is similar to that of ς_1. First, it is direct to show that

$$
\lim_{a \to \underline{a}} \hat{s}_1'(a)\, \hat{s}_1(a) = -\lim_{a \to \underline{a}} c_1'(a)\, \hat{s}_1(a). \quad \text{(A.20)}
$$

By construction,

$$s_1(a) = \hat{s}_1(a) + \sigma k_j(a) h_j(a). \tag{A.21}$$

Plugging it into the Euler equation (A.17) and rearranging yield

$$\begin{aligned} \rho - r &= \frac{v_1''(a)}{v_1'(a)}\left(\hat{s}_1(a) + \sigma k_j(a) h_j(a)\right) + \frac{1}{2}\frac{v_1'''(a)}{v_1'(a)}\sigma^2 k_1^2(a) + \lambda_1\left(\frac{v_2'(a)}{v_1'(a)} - 1\right) \\ &\approx \frac{v_1''(a)\,\hat{s}_1(a)}{v_1'(a)} + \frac{(R-r)^2}{2\sigma^2}\frac{v_1'''(a)\,v_1'(a)}{v_1''(a)^2}\left(1 + 2\varepsilon\left(\begin{array}{c} \frac{v_1'(a)^2}{v_1''(a)} \\ -\frac{v_1'(a)v_1''(a)}{v_1'''(a)} \end{array}\right)\right) \\ &\quad + \lambda_1\left(\frac{v_2'(a)}{v_1'(a)} - 1\right). \end{aligned} \tag{A.22}$$

Using expressions in (A.18) in (A.22) results in

$$\begin{aligned} \rho - r &= -\gamma c_1(a)^{-1} c_1'(a)\,\hat{s}_1(a) - \lambda_1 \gamma c_1(a)^{-1}\left(c_2(a) - c_1(a)\right) \\ &\quad + \frac{1}{2}\left(\frac{R-r}{\sigma}\right)^2\left(\frac{\gamma+1}{\gamma} - \frac{1}{\gamma}c_1(a)\frac{c_1''(a)}{c_1'(a)^2}\right)\left(1 + 2\varepsilon\left(\begin{array}{c} -\frac{1}{\gamma}\frac{c_1(a)^{1-\gamma}}{c_1'(a)} \\ +\frac{c_1(a)^{1-\gamma}c_1'(a)}{(\gamma+1)c_1'(a)^2 - c_1''(a)c_1(a)} \end{array}\right)\right). \end{aligned} \tag{A.23}$$

The combination of equations (A.23) and (A.20) imply that

$$\lim_{a \to \underline{a}} \hat{s}_1'(a)\,\hat{s}_1(a) = \hat{\varsigma}_1,$$

where $\hat{\nu}_1 = \nu_1 - \lambda\varepsilon$, with λ given in (3.9). Since $\hat{s}_1(\underline{a}) = s_1(\underline{a}) = 0$ by (A.21), we reach at

$$\hat{s}_1(a)^2 \approx \hat{s}_1(\underline{a})^2 + 2\hat{s}_1(\underline{a})\,\hat{s}_1'(\underline{a})(a - \underline{a}) = 2\hat{\varsigma}_1(a - \underline{a}),$$

and thus (3.7).

A.3 Proof of Proposition 3

First, we rewrite (A.23) as

$$\begin{aligned} -c_1'(a)\,\hat{s}_1(a) &= \frac{c_1(a)(\rho - r)}{\gamma} + \lambda_1\left(c_2(a) - c_1(a)\right) \\ &\quad - \frac{c_1(a)}{2\gamma}\left(\frac{R-r}{\sigma}\right)^2\left(\frac{\gamma+1}{\gamma} - \frac{1}{\gamma}c_1(a)\frac{c_1''(a)}{c_1'(a)^2}\right)\left(1 + 2\varepsilon\left(\begin{array}{c} -\frac{1}{\gamma}\frac{c_1(a)^{1-\gamma}}{c_1'(a)} \\ +\frac{c_1(a)^{1-\gamma}c_1'(a)}{(\gamma+1)c_1'(a)^2 - c_1''(a)c_1(a)} \end{array}\right)\right). \end{aligned} \tag{A.24}$$

Denote the above equation as

$$\eta(a) = -c_1'(a)\,\hat{s}_1(a) = \eta_1(a) + \eta_2(a) + \eta_3(a), \tag{A.25}$$

where

$$\eta_1(a) = \frac{c_1(a)(\rho - r)}{\gamma} \tag{A.26}$$

$$\eta_2(a) = \lambda_1\left(c_2(a) - c_1(a)\right) \tag{A.27}$$

$$\eta_3(a) = -\frac{c_1(a)}{2\gamma}\left(\frac{R-r}{\sigma}\right)^2 \left(\frac{\gamma+1}{\gamma} - \frac{1}{\gamma} c_1(a)\frac{c_1''(a)}{c_1'(a)^2}\right)\left(1 + 2\varepsilon\left(-\frac{1}{\gamma}\frac{c_1(a)^{1-\gamma}}{c_1'(a)} + \frac{c_1(a)^{1-\gamma}c_1'(a)}{(\gamma+1)c_1'(a)^2 - c_1''(a)c_1(a)}\right)\right) \tag{A.28}$$

Note (3.8) implies $\eta(\underline{a}) = \hat{\varsigma}_1$. Next, we derive in order the first-order approximations of functions $\eta_i(a)$, $i = 1, 2, 3$, around $\varepsilon = 0$. By (A.26), we have

$$\eta_1(a) = \frac{c_1(a)(\rho - r)}{\gamma} \approx \frac{(c_{1,0}(a) + \varepsilon c_{1,1}(a))(\rho - r)}{\gamma} = \eta_{1,0}(a) + \varepsilon \eta_{1,1}(a), \tag{A.29}$$

where

$$\eta_{1,0}(a) = \frac{c_{1,0}(a)(\rho - r)}{\gamma}, \eta_{1,1}(a) = \frac{c_{1,1}(a)(\rho - r)}{\gamma}. \tag{A.30}$$

By the same token, equation (A.27) yields

$$\begin{aligned} \eta_2(a) &= \lambda_1\left(c_2(a) - c_1(a)\right) \approx \lambda_1(c_{2,0}(a) + \varepsilon c_{2,1}(a) - c_{1,0}(a) - \varepsilon c_{1,1}(a)) \\ &= \lambda_1(c_{2,0}(a) - c_{1,0}(a)) + \varepsilon\lambda_1(c_{2,1}(a) - c_{1,1}(a)) = \eta_{2,0}(a) + \varepsilon\eta_{2,1}(a), \end{aligned} \tag{A.31}$$

where

$$\eta_{2,0}(a) = \lambda_1(c_{2,0}(a) - c_{1,0}(a)), \eta_{2,1}(a) = \lambda_1(c_{2,1}(a) - c_{1,1}(a)). \tag{A.32}$$

Finally, we can approximate $\eta_3(a)$ in (A.28) as

$$
\begin{aligned}
\eta_3(a) &= -\frac{c_1(a)}{2\gamma}\left(\frac{R-r}{\sigma}\right)^2\left(\frac{\gamma+1}{\gamma}-\frac{1}{\gamma}c_1\left(a\right)\frac{c_1''\left(a\right)}{c_1'\left(a\right)^2}\right)\left(1+2\varepsilon\begin{pmatrix} -\frac{1}{\gamma}\frac{c_1(a)^{1-\gamma}}{c_1'(a)} \\ +\frac{c_1(a)^{1-\gamma}c_1'(a)}{(\gamma+1)c_1'(a)^2-c_1''(a)c_1(a)}\end{pmatrix}\right) \\
&= -\frac{1}{2\gamma}\left(\frac{R-r}{\sigma}\right)^2\left(\frac{\gamma+1}{\gamma}c_1(a)-\frac{1}{\gamma}c_1\left(a\right)^2\frac{c_1''\left(a\right)}{c_1'\left(a\right)^2}\right)\left(1+2\varepsilon\begin{pmatrix} -\frac{1}{\gamma}\frac{c_1(a)^{1-\gamma}}{c_1'(a)} \\ +\frac{c_1(a)^{1-\gamma}c_1'(a)}{(\gamma+1)c_1'(a)^2-c_1''(a)c_1(a)}\end{pmatrix}\right) \\
&\approx -\frac{1}{2\gamma}\left(\frac{R-r}{\sigma}\right)^2\begin{pmatrix} \frac{(\gamma+1)(c_{1,0}(a)+\varepsilon c_{1,1}(a))}{\gamma} \\ -\frac{1}{\gamma}(c_{1,0}(a)+\varepsilon c_{1,1}(a))^2\frac{c_{1,0}''(a)+\varepsilon c_{1,1}''(a)}{(c_{1,0}'(a)+\varepsilon c_{1,1}'(a))^2}\end{pmatrix} \\
&\quad\times\left(1+2\varepsilon\begin{pmatrix} -\frac{1}{\gamma}\frac{(c_{1,0}(a)+\varepsilon c_{1,1}(a))^{1-\gamma}}{c_{1,0}'(a)+\varepsilon c_{1,1}'(a)} \\ +\frac{(c_{1,0}(a)+\varepsilon c_{1,1}(a))^{1-\gamma}\left(c_{1,0}'(a)+\varepsilon c_{1,1}'(a)\right)}{(\gamma+1)(c_{1,0}'(a)+\varepsilon c_{1,1}'(a))^2-(c_{1,0}''(a)+\varepsilon c_{1,1}''(a))(c_{1,0}'(a)+\varepsilon c_{1,1}'(a))}\end{pmatrix}\right) \\
&\approx \eta_{3,0}(a)+\varepsilon\eta_{3,1}(a),
\end{aligned}
\tag{A.33}
$$

where

$$
\eta_{3,0}(a) = -\frac{1}{2\gamma}\left(\frac{R-r}{\sigma}\right)^2\left(\frac{\gamma+1}{\gamma}c_{1,0}(a)-\frac{1}{\gamma}c_{1,0}(a)^2\frac{c_{1,0}''(a)}{c_{1,0}'\left(a\right)^2}\right), \eta_{3,1}(a) = \eta_{3,0}(a)\tau\left(a\right).
\tag{A.34}
$$

Here the function $\tau\left(a\right)$ is defined as

$$
\begin{aligned}
\tau(a) &= \frac{\theta(a)}{(\gamma+1)c_{1,0}(a)c_{1,0}'\left(a\right)^3-c_{1,0}(a)^2c_{1,0}'(a)c_{1,0}''(a)} \\
&\quad -\frac{2}{\gamma}\frac{c_{1,0}(a)^{1-\gamma}}{c_{1,0}'(a)}+\frac{2c_{1,0}\left(a\right)^{1-\gamma}c_{1,0}'\left(a\right)}{\left(\gamma+1\right)c_{1,0}'\left(a\right)^2-c_{1,0}\left(a\right)c_{1,0}''\left(a\right)}, \\
\theta(a) &= (\gamma+1)c_{1,1}(a)c_{1,0}'(a)^3-\begin{pmatrix} 2c_{1,0}(a)c_{1,1}(a)c_{1,0}''(a) \\ +c_{1,0}(a)^2c_{1,1}''(a)\end{pmatrix}c_{1,0}'(a)+2c_{1,0}(a)^2c_{1,0}''(a)c_{1,1}'(a).
\end{aligned}
$$

Substituting (A.29), (A.31) and (A.33) into (A.25) and taking the limit of a to $\underline{a}$ lead to

$$
\begin{aligned}
\hat{\varsigma}_1 &= \lim_{a\to\underline{a}}\eta\left(a\right) = \lim_{a\to\underline{a}}\sum_{i=1}^{3}\eta_i\left(a\right) \approx \lim_{a\to\underline{a}}\sum_{i=1}^{3}\left(\eta_{i,0}\left(a\right)+\varepsilon\eta_{i,1}\left(a\right)\right) \\
&= \sum_{i=1}^{3}\eta_{i,0}\left(\underline{a}\right)+\varepsilon\sum_{i=1}^{3}\eta_{i,1}\left(\underline{a}\right).
\end{aligned}
\tag{A.35}
$$

Note that

$$\sum_{i=1}^{3} \eta_{i,0}\left(\underline{a}\right) = \left(\begin{array}{c} \frac{c_{1,0}(\underline{a})(\rho-r)}{\gamma} + \lambda_1(c_{2,0}(\underline{a}) - c_{1,0}(\underline{a})) \\ -\frac{1}{2\gamma}\left(\frac{R-r}{\sigma}\right)^2 \left(\frac{(\gamma+1)c_{1,0}(\underline{a})}{\gamma} - \frac{1}{\gamma}c_{1,0}(\underline{a})^2 \frac{c''_{1,0}(\underline{a})}{c'_{1,0}(\underline{a})^2}\right) \end{array} \right) = \varsigma_{1,0}. \tag{A.36}$$

Combining (A.35) and (A.36) yields (3.10) as desired, where

$$\varsigma_{1,1} = \sum_{i=1}^{3} \eta_{i,1}\left(\underline{a}\right). \tag{A.37}$$

A.4 Proof of Proposition 4

To prove (3.13), by (3.10) it suffices to show $\varsigma_{1,1} > 0$. Because $c_{1,1}(\underline{a}) > 0$, we have

$$\eta_{1,1}\left(\underline{a}\right) = \frac{c_{1,1}(\underline{a})(\rho - r)}{\gamma} > 0.$$

Meanwhile, the condition $c_{2,1}\left(\underline{a}\right) > c_{1,1}\left(\underline{a}\right)$ implies that

$$\eta_{2,1}(\underline{a}) = \lambda_1(c_{2,1}(\underline{a}) - c_{1,1}(\underline{a})) > 0.$$

Since $c''_{1,0}(a) < 0$, $\eta_{3,0}\left(\underline{a}\right) < 0$ by (A.34). Furthermore, given $\theta(\underline{a}) < 0$ and $c'_{1,0}(a) > 0$, we have $\tau\left(\underline{a}\right) < 0$ and thus

$$\eta_{3,1}(\underline{a}) = \eta_{3,0}(\underline{a})\tau\left(\underline{a}\right) > 0.$$

implying $\varsigma_{1,1} = \sum_{i=1}^{3} \eta_{i,1}\left(\underline{a}\right) > 0$. Employing (3.13) and the two approximations (3.7) and (3.12) yields the relationship in (3.14).

A.5 Proof of Lemma 1

Suppose equation (3.15) holds, it follows that

$$v'_j\left(a\right) \approx v'_{j,0}\left(a\right) + \varepsilon v'_{j,1}\left(a\right), v''_j\left(a\right) \approx v''_{j,0}\left(a\right) + \varepsilon v''_{j,1}\left(a\right). \tag{A.38}$$

Therefore, by (A.9), we have

$$\begin{aligned}
c_j(a) &= v_j'(a)^{-\frac{1}{\gamma}} \approx \left(v_{j,0}'(a) + \varepsilon v_{j,1}'(a)\right)^{-\frac{1}{\gamma}} \\
&= v_{j,0}'(a)^{-\frac{1}{\gamma}} \left(1 + \varepsilon \frac{v_{j,1}'(a)}{v_{j,0}'(a)}\right)^{-\frac{1}{\gamma}} \\
&\approx v_{j,0}'(a)^{-\frac{1}{\gamma}} \left(1 - \varepsilon \frac{1}{\gamma} \frac{v_{j,1}'(a)}{v_{j,0}'(a)}\right) \\
&= c_{j,0}(a) + \varepsilon c_{j,1}(a),
\end{aligned} \tag{A.39}$$

where

$$c_{j,0}(a) = v_{j,0}'(a)^{-\frac{1}{\gamma}}, \; c_{j,1}(a) = -\frac{1}{\gamma} v_{j,0}'(a)^{-\frac{1}{\gamma}-1} v_{j,1}'(a). \tag{A.40}$$

Equations (A.10) and (A.11) imply that

$$\begin{aligned}
k_j(a) &= \frac{R-r}{\sigma^2} \frac{v_j'(a)}{\varepsilon v_j'(a)^2 - v_j''(a)} \\
&\approx \frac{R-r}{\sigma^2} \left(-\frac{v_j'(a)}{v_j''(a)} - \varepsilon \frac{v_j'(a)^3}{v_j''(a)^2}\right) \\
&\approx \frac{R-r}{\sigma^2} \left(-\frac{v_{j,0}'(a) + \varepsilon v_{j,1}'(a)}{v_{j,0}''(a) + \varepsilon v_{j,1}''(a)} - \varepsilon \frac{\left(v_{j,0}'(a) + \varepsilon v_{j,1}'(a)\right)^3}{\left(v_{j,0}''(a) + \varepsilon v_{j,1}''(a)\right)^2}\right) \\
&\approx k_{j,0}(a) + \varepsilon k_{j,1}(a),
\end{aligned} \tag{A.41}$$

where

$$k_{j,0}(a) = -\frac{R-r}{\sigma^2} \frac{v_{j,0}'(a)}{v_{j,0}''(a)}, k_{j,1}(a) = -\frac{R-r}{\sigma^2} \frac{v_{j,1}'(a) v_{j,0}''(a) + v_{j,0}'(a) \left(v_{j,0}'(a)^2 - v_{j,1}''(a)\right)}{v_{j,0}''(a)^2}. \tag{A.42}$$

Similarly, we have

$$\begin{aligned}
h_j(a) &= -\frac{R-r}{\sigma} \frac{\varepsilon v_j'(a)^2}{\varepsilon v_j'(a)^2 - v_j''(a)} \\
&\approx -\frac{R-r}{\sigma} \frac{\varepsilon \left(v_{j,0}'(a) + \varepsilon v_{j,1}'(a)\right)^2}{\varepsilon \left(v_{j,0}'(a) + \varepsilon v_{j,1}'(a)\right)^2 - \left(v_{j,0}''(a) + \varepsilon v_{j,1}''(a)\right)} \\
&\approx \varepsilon h_{j,1}(a),
\end{aligned} \tag{A.43}$$

where

$$h_{j,1}(a) = \frac{R-r}{\sigma} \frac{v'_{j,0}(a)^2}{v''_{j,0}(a)}. \tag{A.44}$$

Substituting (3.15), (A.38), (A.39), (A.41) and (A.43) into both sides of equation (3.3), and collecting terms with the same ε power yield that $v_{j,0}(a)$ and $v_{j,1}(a)$ satisfy the following two coupled functional equations:

$$\begin{aligned}
\rho v_{j,0}(a) &= \frac{c_{j,0}(a)^{1-\gamma}}{1-\gamma} + v'_{j,0}(a)\left(wz_j + ra + k_{j,0}(a)(R-r) - c_{j,0}(a)\right) && \text{(A.45)} \\
&\quad + \frac{1}{2}\sigma^2 v''_{j,0}(a) k^2_{j,0}(a) + \lambda_j\left(v_{-j,0}(a) - v_{j,0}(a)\right), \\
\rho v_{j,1}(a) &= c_{j,0}(a)^{-\gamma} c_{j,1}(a) + v'_{j,0}(a)\left(k_{j,1}(a)(R-r) - c_{j,1}(a)\right) && \text{(A.46)} \\
&\quad + v'_{j,1}(a)\left(wz_j + ra + k_{j,0}(a)(R-r) - c_{j,0}(a)\right) \\
&\quad + \sigma^2\left(v''_{j,0}(a) k_{j,0}(a) k_{j,1}(a) + \frac{1}{2} v''_{j,1}(a) k^2_{j,0}(a)\right) \\
&\quad - \frac{1}{2}\sigma^2 v'_{j,0}(a)^2 k_{j,0}(a)^2 + \lambda_j\left(v_{-j,1}(a) - v_{j,1}(a)\right).
\end{aligned}$$

Next, we prove the homogeneity results. By (3.16), we have

$$v_{j,0}(a) = \xi^{1-\gamma} v_{\xi,j,0}\left(\frac{a}{\xi}\right), v_{j,1}(a) = \xi^{2(1-\gamma)} v_{\xi,j,1}\left(\frac{a}{\xi}\right),$$

and thus

$$\begin{aligned}
v'_{j,0}(a) &= \xi^{-\gamma} v'_{\xi,j,0}\left(\frac{a}{\xi}\right), v'_{j,1}(a) = \xi^{1-2\gamma} v'_{\xi,j,1}\left(\frac{a}{\xi}\right), \\
v'_{j,0}(a) &= \xi^{-\gamma-1} v'_{\xi,j,0}\left(\frac{a}{\xi}\right), v''_{j,1}(a) = \xi^{-2\gamma} v_{\xi,j,1}\left(\frac{a}{\xi}\right).
\end{aligned}$$

It then follows from (A.40), (A.42) and (A.44) that

$$
\begin{aligned}
c_{j,0}(a) &= v'_{j,0}(a)^{-\frac{1}{\gamma}} = \left(\xi^{-\gamma} v'_{\xi,j,0}\left(\frac{a}{\xi}\right)\right)^{-\frac{1}{\gamma}} = \xi\left(v'_{\xi,j,0}\left(\frac{a}{\xi}\right)\right)^{-\frac{1}{\gamma}} = \xi c_{\xi,j,0}\left(\frac{a}{\xi}\right) && \text{(A.47)}\\
c_{j,1}(a) &= -\frac{1}{\gamma} v'_{j,0}(a)^{-\frac{1}{\gamma}-1} v'_{j,1}(a) = -\frac{1}{\gamma}\left(\xi^{-\gamma} v'_{\xi,j,0}\left(\frac{a}{\xi}\right)\right)^{-\frac{1}{\gamma}-1} \xi^{1-2\gamma} v'_{\xi,j,1}\left(\frac{a}{\xi}\right) \\
&= -\xi^{2-\gamma}\frac{1}{\gamma} v'_{\xi,j,0}\left(\frac{a}{\xi}\right)^{-\frac{1}{\gamma}-1} v'_{\xi,j,1}\left(\frac{a}{\xi}\right) = \xi^{2-\gamma} c_{\xi,j,1}\left(\frac{a}{\xi}\right) && \text{(A.48)}\\
k_{j,0}(a) &= -\frac{R-r}{\sigma^2}\frac{v'_{j,0}(a)}{v''_{j,0}(a)} = -\frac{R-r}{\sigma^2}\frac{\xi^{-\gamma} v'_{\xi,j,0}\left(\frac{a}{\xi}\right)}{\xi^{-\gamma-1} v'_{\xi,j,0}\left(\frac{a}{\xi}\right)} = \xi k_{\xi,j,0}\left(\frac{a}{\xi}\right) && \text{(A.49)}\\
k_{j,1}(a) &= -\frac{R-r}{\sigma^2}\frac{v'_{j,1}(a)\, v''_{j,0}(a) + v'_{j,0}(a)\left(v'_{j,0}(a)^2 - v''_{j,1}(a)\right)}{\left(v''_{j,0}(a)\right)^2} = \xi^{2-\gamma} k_{\xi,j,1}\left(\frac{a}{\xi}\right) && \text{(A.50)}\\
h_{j,1}(a) &= \frac{R-r}{\sigma}\frac{v'_{j,0}(a)^2}{v''_{j,0}(a)} = \frac{R-r}{\sigma}\frac{\left(\xi^{-\gamma} v'_{\xi,j,0}\left(\frac{a}{\xi}\right)\right)^2}{\xi^{-2\gamma} v_{\xi,j,1}\left(\frac{a}{\xi}\right)} = \xi^{1-\gamma} h_{\xi,j,1}\left(\frac{a}{\xi}\right). && \text{(A.51)}
\end{aligned}
$$

By inserting (A.47) to (A.51) into both (A.45) and (A.46) and rearranging terms, we obtain that $v_{\xi,j,0}(a)$ and $v_{\xi,j,1}(a)$ satisfy the following two coupled functional equations:

$$
\begin{aligned}
\rho v_{\xi,j,0}(a) &= \frac{c_{\xi,j,0}(a)^{1-\gamma}}{1-\gamma} + v'_{\xi,j,0}(a)\left(\frac{wz_j}{\xi} + ra + k_{\xi,j,0}(a)(R-r) - c_{\xi,j,0}(a)\right) && \text{(A.52)}\\
&\quad + \frac{1}{2}\sigma^2 v''_{\xi,j,0}(a)\, k^2_{\xi,j,0}(a) + \lambda_j\left(v_{\xi,-j,0}(a) - v_{\xi,j,0}(a)\right), \\
\rho v_{\xi,j,1}(a) &= c_{\xi,j,0}(a)^{-\gamma} c_{\xi,j,1}(a) + v'_{\xi,j,0}(a)\left(k_{\xi,j,1}(a)(R-r) - c_{\xi,j,1}(a)\right) && \text{(A.53)}\\
&\quad + v'_{\xi,j,1}(a)\left(\frac{wz_j}{\xi} + ra + k_{\xi,j,0}(a)(R-r) - c_{\xi,j,0}(a)\right) \\
&\quad + \sigma^2\left(v''_{\xi,j,0}(a)\, k_{\xi,j,0}(a)\, k_{\xi,j,1}(a) + \frac{1}{2} v''_{\xi,j,1}(a)\, k^2_{\xi,j,0}(a)\right) \\
&\quad - \frac{1}{2}\sigma^2 v'_{\xi,j,0}(a)^2\, k_{\xi,j,0}(a)^2 + \lambda_j\left(v_{\xi,-j,1}(a) - v_{\xi,j,1}(a)\right),
\end{aligned}
$$

where in (A.52) and (A.53) we define

$$c_{\xi,j,0}\left(a\right)=v'_{\xi,j,0}\left(a\right)^{-\frac{1}{\gamma}},c_{\xi,j,1}\left(a\right)=-\frac{1}{\gamma}v'_{\xi,j,0}\left(a\right)^{-\frac{1}{\gamma}-1}v'_{\xi,j,1}\left(a\right), \tag{A.54}$$

$$k_{\xi,j,0}\left(a\right)=-\frac{R-r}{\sigma^2}\frac{v'_{\xi,j,0}\left(a\right)}{v''_{\xi,j,0}\left(a\right)},k_{\xi,j,0}\left(a\right)=-\frac{R-r}{\sigma^2}\frac{\left(\begin{array}{c}v'_{\xi,j,1}\left(a\right)v''_{\xi,j,0}\left(a\right)\\+v'_{\xi,j,0}\left(a\right)\left(v'_{\xi,j,0}\left(a\right)^2-v''_{\xi,j,1}\left(a\right)\right)\end{array}\right)}{v''_{\xi,j,0}\left(a\right)^2}. \tag{A.55}$$

A.6 Proof of Proposition 5

By Lemma 1, we have for any $a\in(\underline{a},\infty)$,

$$\lim_{\xi\to\infty}v_{\xi,j,0}\left(a\right)=\tilde{v}_0\left(a\right),\ \lim_{\xi\to\infty}v_{\xi,j,1}\left(a\right)=\tilde{v}_1\left(a\right), \tag{A.56}$$

where $\tilde{v}_0\left(a\right)$ and $\tilde{v}_1\left(a\right)$ solve the following two functional equations

$$\begin{aligned}
\rho\tilde{v}_0\left(a\right) &= \frac{\tilde{c}_0\left(a\right)^{1-\gamma}}{1-\gamma}+\tilde{v}'_0\left(a\right)\left(ra+\tilde{k}_0\left(a\right)\left(R-r\right)-\tilde{c}_0\left(a\right)\right)+\frac{1}{2}\sigma^2\tilde{v}''_0\left(a\right)\tilde{k}_0^2\left(a\right) && \text{(A.57)}\\
\rho\tilde{v}_1\left(a\right) &= \tilde{c}_0\left(a\right)^{-\gamma}\tilde{c}_1\left(a\right)+\tilde{v}'_0\left(a\right)\left(\tilde{k}_1\left(a\right)\left(R-r\right)-\tilde{c}_1\left(a\right)\right) && \text{(A.58)}\\
&\quad+\tilde{v}'_1\left(a\right)\left(ra+\tilde{k}_0\left(a\right)\left(R-r\right)-\tilde{c}_0\left(a\right)\right)\\
&\quad+\sigma^2\left(\tilde{v}''_0\left(a\right)\tilde{k}_0\left(a\right)\tilde{k}_1\left(a\right)+\frac{1}{2}\tilde{v}''_1\left(a\right)\tilde{k}_0^2\left(a\right)\right)-\frac{1}{2}\sigma^2\tilde{v}'_0\left(a\right)^2\tilde{k}_0\left(a\right)^2,
\end{aligned}$$

with

$$\tilde{c}_0\left(a\right)=\tilde{v}'_0\left(a\right)^{-\frac{1}{\gamma}},\tilde{c}_1\left(a\right)=-\frac{1}{\gamma}\tilde{v}'_0\left(a\right)^{-\frac{1}{\gamma}-1}\tilde{v}'_1\left(a\right) \tag{A.59}$$

$$\tilde{k}_0\left(a\right)=-\frac{R-r}{\sigma^2}\frac{\tilde{v}'_0\left(a\right)}{\tilde{v}''_0\left(a\right)},\tilde{k}_1\left(a\right)=-\frac{R-r}{\sigma^2}\frac{\tilde{v}'_1\left(a\right)\tilde{v}''_0\left(a\right)+\tilde{v}'_0\left(a\right)\left(\tilde{v}'_0\left(a\right)^2-\tilde{v}''_1\left(a\right)\right)}{\tilde{v}''_0\left(a\right)^2} \tag{A.60}$$

$$\tilde{h}_1\left(a\right)=\frac{R-r}{\sigma}\frac{\tilde{v}'_0\left(a\right)^2}{\tilde{v}''_0\left(a\right)}. \tag{A.61}$$

It is straightforward to verify that $\tilde{v}\left(a\right)=\tilde{v}_1\left(a\right)+\varepsilon\tilde{v}_0\left(a\right)$ is an approximate solution to the HJB equation (3.3) absent income uncertainty and borrowing constraint. Combining equation (A.47) with (A.56) leads to that for a very large,

$$c_{j,0}\left(a\right)=\xi c_{\xi,j,0}\left(\frac{a}{\xi}\right)=ac_{a,j,0}\left(1\right)\approx a\tilde{c}_0\left(1\right). \tag{A.62}$$

Similarly, we have

$$\begin{aligned} c_{j,1}(a) &= \xi^{2-\gamma} c_{\xi,j,1}\left(\frac{a}{\xi}\right) = a^{2-\gamma} c_{a,j,1}(1) \approx a^{2-\gamma} \tilde{c}_1(1) && \text{(A.63)} \\ k_{j,0}(a) &= \xi k_{\xi,j,0}\left(\frac{a}{\xi}\right) = \xi k_{a,j,0}(1) \approx a \tilde{k}_0(1) && \text{(A.64)} \\ k_{j,1}(a) &= \xi^{2-\gamma} k_{\xi,j,1}\left(\frac{a}{\xi}\right) = a^{2-\gamma} k_{a,j,1}(1) \approx a^{2-\gamma} \tilde{k}_1(1) && \text{(A.65)} \\ h_{j,1}(a) &= \xi^{1-\gamma} h_{\xi,j,1}\left(\frac{a}{\xi}\right) = a^{1-\gamma} h_{a,j,1}(1) \approx a^{1-\gamma} \tilde{h}_1(1). && \text{(A.66)} \end{aligned}$$

Therefore, it remains to solve equations (A.57) and (A.58). First, conjecture

$$\tilde{v}_0(a) = \alpha_0 \frac{a^{1-\gamma}}{1-\gamma} \tag{A.67}$$

for some number α_0. In this case, we have $\tilde{v}_0'(a) = \alpha_0 a^{-\gamma}$, $\tilde{v}_0''(a) = -\gamma\alpha_0 a^{-\gamma-1}$, and subsequently from equations (A.59) to (A.61) that

$$\tilde{c}_0(a) = \alpha_0^{-\frac{1}{\gamma}} a,\ \tilde{k}_0(a) = \frac{R-r}{\sigma^2} a,\ \tilde{h}_1(a) = -\frac{R-r}{\sigma^2}\alpha_0 a^{1-\gamma}. \tag{A.68}$$

Inserting (A.67) and (A.68) into (A.57) gives the value of α_0:

$$\alpha_0 = \left(\frac{\rho-(1-\gamma)r}{\gamma} - \frac{1-\gamma}{2\gamma}\frac{(R-r)^2}{\gamma\sigma^2}\right)^{-\gamma}. \tag{A.69}$$

Next, conjecture

$$\tilde{v}_1(a) = \alpha_1 \frac{a^{2(1-\gamma)}}{2(1-\gamma)} \tag{A.70}$$

for some number α_1. Thus, we have $\tilde{v}_1'(a) = \alpha_1 a^{1-2\gamma}$, $\tilde{v}_1''(a) = (1-2\gamma)\alpha_1 a^{1-2\gamma}$, and subsequently from (A.59) to (A.61) that

$$\tilde{c}_1(a) = -\frac{1}{\gamma}\alpha_0^{-\frac{1}{\gamma}-1}\alpha_1 a^{2-\gamma},\ \tilde{k}_1(a) = -\frac{R-r}{\sigma^2}\frac{\alpha_0^2+(\gamma-1)\alpha_1}{\gamma^2\alpha_0} a^{2-\gamma}. \tag{A.71}$$

Substituting (A.70) and (A.71) into (A.58) results in

$$\alpha_1\left(r - \alpha_0^{-\frac{1}{\gamma}} + \frac{1}{2}\frac{(R-r)^2}{\gamma^2\sigma^2} - \frac{\rho}{2(1-\gamma)}\right) = -\frac{1}{2}\alpha_0^2\frac{(R-r)^2}{\gamma^2\sigma^2},$$

and thus the value of α_1:

$$\alpha_1 \quad = \quad \frac{\frac{1}{2}\alpha_0^2\left(\frac{R-r}{\gamma\sigma}\right)^2}{r-\alpha_0^{-\frac{1}{\gamma}}+\frac{1}{2}\left(\frac{R-r}{\gamma\sigma}\right)^2-\frac{\rho}{2(1-\gamma)}}. \tag{A.72}$$

By (A.39), (A.62) and (A.63), when a is sufficiently large, we have

$$c_j\left(a\right)\approx c_{j,0}\left(a\right)+\varepsilon c_{j,1}\left(a\right)\approx a\tilde{c}_0\left(1\right)+\varepsilon a^{2-\gamma}\tilde{c}_1\left(1\right)=\alpha_0^{-\frac{1}{\gamma}}a-\varepsilon\frac{1}{\gamma}\alpha_0^{-\frac{1}{\gamma}-1}\alpha_1 a^{2-\gamma}.$$

By the same token,

$$k_j\left(a\right)\approx k_{j,0}\left(a\right)+\varepsilon k_{j,1}\left(a\right)\approx a\tilde{k}_0\left(1\right)+\varepsilon a^{2-\gamma}\tilde{k}_1\left(1\right)=\frac{R-r}{\sigma^2}a-\varepsilon\frac{R-r}{\sigma^2}\frac{\alpha_0^2+\left(\gamma-1\right)\alpha_1}{\gamma^2\alpha_0}a^{2-\gamma}$$

$$h_j\left(a\right)\approx\varepsilon h_{j,1}\left(a\right)\approx\varepsilon a^{1-\gamma}\tilde{h}_1\left(1\right)=-\varepsilon\frac{R-r}{\sigma^2}\alpha_0 a^{1-\gamma}.$$

A.7 Proof of Proposition 6

The borrowing constraint $0\leq k_j\left(a\right)\leq a-\underline{a}$ implies that $\lim_{a\to\underline{a}}k_j\left(a\right)=0$, and then by (3.22) and (A.9)

$$\lim_{a\to\underline{a}}h_j\left(a\right)=-\lim_{a\to\underline{a}}\varepsilon\sigma k_j\left(a\right)v_j'\left(a\right)=-\lim_{a\to\underline{a}}\varepsilon\sigma k_j\left(a\right)u'\left(c_j(a)\right)=0,$$

where the last equality rests on that $c_2(\underline{a})\geq c_1(\underline{a})=wz_1+r\underline{a}>0$ and thus $\lim_{a\to\underline{a}}u'\left(c_j\left(a\right)\right)<\infty$. The second limit in (3.20) takes advantage of the approximation (3.19). Finally, applying the Rolle's theorem to $h_j(a)$ with (3.20) guarantees the existence of a_j^* in (3.21).

B Numerical algorithm

This paper computes the perceived law of motion (4.1) using approximation techniques proposed in Krusell and Smith (1997) and Achdou et al. (2022). The numerical algorithm comprises the following steps:

1. Guess initial forecasting coefficients β^0 for the PLM of capital stock and interest rate as specified in (4.1) and (4.2).

2. Using the guess in Step 1, solve the HJB equation (4.3) using an upward finite difference method.

3. Apply the value and policy functions obtained in Step 2 to simulate the dynamics of capital stock and interest rate with a constant time step Δt:

   (a) Choose the initial density $g_1 = g_{ss}$, capital stock $K_1 = K_{ss}$, and volatility $\vartheta_1 = \bar{\vartheta}$, where g_{ss} and K_{ss} denote, respectively, the density function and aggregate capital in the stationary equilibrium, and draw a sequence of aggregate volatility $\{\vartheta_t\}_{t=1}^{T}$ by (2.5) using a random number generator.

   (b) Since the forecasting rule of the interest rate in (4.1) might not exactly clear the bond market at all dates and states, we solve an additional optimization problem at each point in time in the simulation, a scheme similar to Krusell and Smith (1997). More precisely, at time t, observing the density g_t, aggregate capital $K_t = \sum_{i,j} a_i g_t(a_i, z_j)$, and aggregate volatility ϑ_t, given a guessed interest rate r_0, solve the following optimization problem for households of state (a_i, z_j):

$$
\begin{aligned}
&\max_{c,k} \min_{h} \frac{c^{1-\gamma}}{1-\gamma} + \frac{1}{2\varepsilon}h^2 + s(a_i, z_j, K_t, \vartheta_t)\frac{\partial v}{\partial a} + \frac{\vartheta_t k^2}{2}\frac{\partial^2 v}{\partial a^2} \\
&+ \lambda_j(v(a_i, z_{-j}, K_t, \vartheta_t) - v(a_i, z_j, K_t, \vartheta_t)) + p(K_t, \vartheta_t)\frac{\partial v}{\partial K} \\
&+ \theta(\bar{\vartheta} - \vartheta_t)\frac{\partial v}{\partial \vartheta} + \frac{\vartheta_t \nu^2}{2}\frac{\partial^2 v}{\partial \vartheta^2},
\end{aligned} \tag{B.1}
$$

   subject to the same constraints for problem (4.3). Here v is the value function as solved in Step (2), and $s(a, z_j, K_t, \vartheta_t) = w_t z_j + r_0 a + (R_t - r_0 + \sqrt{\vartheta_t} h)k - c$ is the perceived saving rate associated with the guessed interest rate r_0. This gives the household's optimal risky investment $k^{(r^0)}(a, z_j)$. Look for r_0 such that the implied aggregate capital $K^{(r^0)} = \sum_{j=1}^{2} \int k^{(r^0)}(a, z_j) g_t(a, z_j)$ equals K_t, i.e., the bond market is cleared. Apply the KF equation to derive the next-period distribution g_{t+1} and capital stock K_{t+1}.

   (c) Keep implementing the above procedure with the provided random draws and get a series $\{\vartheta_t, g_t, K_t, r_t\}_{t=1}^{T}$.

4. Run OLS using the simulated series and obtain the new forecasting coefficients β^1. If new coefficients are close enough to the previous ones, then the iteration over coefficients is finished. Otherwise, update the coefficients by $\beta^0 = (1-\kappa)\beta^0 + \kappa\beta^1$ for some $\kappa \in (0, 1)$ and go back to Step (2).

5. Upon convergence of the coefficients, check the goodness of fit. If it is not satisfactory, try different functional forms for the forecasting functions or add more moments of the distribution.

We next describe in details the steps involved in solving the HJB and KF equations.

B.1 Solving the HJB equation

We first discretize the state space of (a, z_j, K, ϑ) on a finite uniform grid of size $(I, 2, L, M)$ with step sizes Δa, ΔK and $\Delta \vartheta$, respectively. The model is approximated over $a \in \{a_1, \cdots, a_I\}$, where $a_i = a_1 + (i-1)\Delta a$ for $2 \leq i \leq I$, and similarly for $K \in \{K_1, \cdots, K_L\}$, and $\vartheta \in \{\vartheta_1, \cdots, \vartheta_M\}$. The four-dimensional arrays are then used to store the value and policy functions.

For ease of exposition, we denote $v_{i,j,l,m} = v(a_i, z_j, K_l, \vartheta_m)$, and similarly for policy functions $c_{i,j,l,m}$, $k_{i,j,l,m}$ and $h_{i,j,l,m}$ for $i = 1, \cdots, I$, $j = 1, 2$, $l = 1, \cdots, L$, $m = 1, \cdots, M$. The derivatives with respect to individual wealth are approximated as

$$
\begin{aligned}
\frac{\partial v(a_i, z_j, K_l, \vartheta_m)}{\partial a} &\approx \partial_{a,F} v_{i,j,l,m} = \frac{v_{i+1,j,l,m} - v_{i,j,l,m}}{\Delta a} \\
\frac{\partial v(a_i, z_j, K_l, \vartheta_m)}{\partial a} &\approx \partial_{a,B} v_{i,j,l,m} = \frac{v_{i,j,l,m} - v_{i-1,j,l,m}}{\Delta a} \\
\frac{\partial^2 v(a_i, z_j, K_l, \vartheta_m)}{\partial a^2} &\approx \partial_{aa} v_{i,j,l,m} = \frac{v_{i+1,j,l,m} - 2v_{i,j,l,m} + v_{i-1,j,l,m}}{(\Delta a)^2},
\end{aligned}
$$

whereas that with respect to aggregate state variables are

$$
\begin{aligned}
\frac{\partial v(a_i, z_j, K_l, \vartheta_m)}{\partial K} &\approx \partial_{K,F} v_{i,j,l,m} = \frac{v_{i,j,l+1,m} - v_{i,j,l,m}}{\Delta K} \\
\frac{\partial v(a_i, z_j, K_l, \vartheta_m)}{\partial K} &\approx \partial_{K,B} v_{i,j,l,m} = \frac{v_{i,j,l,m} - v_{i,j,l-1,m}}{\Delta K} \\
\frac{\partial v(a_i, z_j, K_l, \vartheta_m)}{\partial \vartheta} &\approx \partial_{\vartheta,F} v_{i,j,l,m} = \frac{v_{i,j,l,m+1} - v_{i,j,l,m}}{\Delta \vartheta} \\
\frac{\partial v(a_i, z_j, K_l, \vartheta_m)}{\partial \vartheta} &\approx \partial_{\vartheta,B} v_{i,j,l,m} = \frac{v_{i,j,l,m} - v_{i,j,l,m-1}}{\Delta \vartheta} \\
\frac{\partial^2 v(a_i, z_j, K_l, \vartheta_m)}{\partial \vartheta^2} &\approx \partial_{\vartheta\vartheta} v_{i,j,l,m} = \frac{v_{i,j,l,m+1} - 2v_{i,j,l,m} + v_{i,j,l,m-1}}{(\Delta \vartheta)^2}.
\end{aligned}
$$

Using these approximated derivatives, the HJB equation (4.3) becomes

$$\begin{aligned}\frac{v_{i,j,l,m}^{d+1}-v_{i,j,l,m}^{d}}{\Delta}+\rho v_{i,j,l,m}^{d+1}=&\frac{(c_{i,j,l,m}^{d})^{1-\gamma}}{1-\gamma}+\frac{1}{2\varepsilon}(h_{i,j,l,m}^{d})^{2}+[s_{i,j,l,m,F}^{d}]^{+}\partial_{a,F}v_{i,j,l,m}^{d+1}+[s_{i,j,l,m,B}^{d}]^{-}\partial_{a,B}v_{i,j,l,m}^{d+1}\\&+\lambda_{j}(v_{i,-j,l,m}^{d+1}-v_{i,j,l,m}^{d+1})+\frac{\vartheta_{m}(k_{i,j,l,m}^{d})^{2}}{2}\partial_{aa}v_{i,j,l,m}^{d+1}\\&+[p_{l,m}]^{+}\partial_{K,F}v_{i,j,l,m}^{d+1}+[p_{l,m}]^{-}\partial_{K,B}v_{i,j,l,m}^{d+1}\\&+[\theta(\bar{\vartheta}-\vartheta_{m})]^{+}\partial_{\vartheta,F}v_{i,j,l,m}^{d+1}+[\theta(\bar{\vartheta}-\vartheta_{m})]^{-}\partial_{\vartheta,B}v_{i,j,l,m}^{d+1}+\frac{\vartheta_{m}\nu^{2}}{2}\partial_{\vartheta\vartheta}v_{i,j,l,m}^{d+1},\end{aligned}\tag{B.2}$$

where $c_{i,j,l,m}^{d}=(\partial_{a}v_{i,j,l,m}^{d})^{-\frac{1}{\gamma}}$, $k_{i,j,l,m}^{d}=-\frac{\partial_{a}v_{i,j,l,m}^{d}}{\partial_{aa}v_{i,j,l,m}^{d}}\frac{\pi_{i,j,l,m}}{\vartheta_{m}}$, $h_{i,j,l,m}^{d}=-\varepsilon\sqrt{\vartheta_{m}}k_{i,j,l,m}^{d}\partial_{a}v_{i,j,l,m}^{d}$, and

$$\begin{aligned}s_{i,j,l,m,F}^{d}&=w_{l,m}z_{j}+r_{l,m}a_{i}+(R_{l,m}-r_{l,m}+\sqrt{\vartheta_{m}}h_{i,j,l,m}^{d})k_{i,j,l,m}^{d}-(\partial_{a,F}v_{i,j,l,m}^{d})^{-\frac{1}{\gamma}}\\s_{i,j,l,m,B}^{d}&=w_{l,m}z_{j}+r_{l,m}a_{i}+(R_{l,m}-r_{l,m}+\sqrt{\vartheta_{m}}h_{i,j,l,m}^{d})k_{i,j,l,m}^{d}-(\partial_{a,B}v_{i,j,l,m}^{d})^{-\frac{1}{\gamma}}.\end{aligned}\tag{B.3}$$

For a generic variable x, we denote $[x]^{+}=\max\{x,0\}$ and $[x]^{-}=\min\{x,0\}$ as the positive and negative parts of x, respectively. In (B.2), when evaluating optimal policies, we use

$$\partial_{a}v_{i,j,l,m}^{d}=\partial_{a,F}v_{i,j,l,m}^{d}\mathbf{1}_{s_{i,j,l,m,F}^{d}>0}+\partial_{a,B}v_{i,j,l,m}^{d}\mathbf{1}_{s_{i,j,l,m,B}^{d}<0}+\partial_{a}\bar{v}_{i,j,l,m}^{d}\mathbf{1}_{s_{i,j,l,m,F}^{d}\leq 0\leq s_{i,j,l,m,B}^{d}},\tag{B.4}$$

where $\partial_{a}\bar{v}_{i,j,l,m}^{d}=(\bar{c}_{i,j,l,m})^{-\gamma}$ with $\bar{c}_{i,j,l,m}$ denoting the steady-state consumption such that $s_{i,j,l,m}^{d}=0$, i.e.,

$$\bar{c}_{i,j,l,m}=w_{l,m}z_{j}+r_{l,m}a_{i}+(R_{l,m}-r_{l,m}+\sqrt{\vartheta_{m}}h_{i,j,l,m}^{d})k_{i,j,l,m}^{d}.\tag{B.5}$$

Employing the approximated derivatives gives

$$
\begin{aligned}
\frac{v^{d+1}_{i,j,l,m} - v^{d}_{i,j,l,m}}{\Delta} + \rho v^{d+1}_{i,j,l,m} =& \frac{(c^{d}_{i,j,l,m})^{1-\gamma}}{1-\gamma} + \frac{1}{2\varepsilon}(h^{d}_{i,j,l,m})^2 + [s^{d}_{i,j,l,m,F}]^{+}\frac{v^{d+1}_{i+1,j,l,m} - v^{d+1}_{i,j,l,m}}{\Delta a} \\
&+ [s^{d}_{i,j,l,m,B}]^{-}\frac{v^{d+1}_{i,j,l,m} - v^{d+1}_{i-1,j,l,m}}{\Delta a} + \lambda_j(v^{d+1}_{i,-j,l,m} - v^{d+1}_{i,j,l,m}) \\
&+ \frac{\vartheta_m (k^{d}_{i,j,l,m})^2}{2}\frac{v^{d+1}_{i+1,j,l,m} - 2v^{d+1}_{i,j,l,m} + v^{d+1}_{i-1,j,l,m}}{(\Delta a)^2} \\
&+ [p_{l,m}]^{+}\frac{v^{d+1}_{i,j,l+1,m} - v^{d+1}_{i,j,l,m}}{\Delta K} + [p_{l,m}]^{-}\frac{v^{d+1}_{i,j,l,m} - v^{d+1}_{i,j,l-1,m}}{\Delta K} \\
&+ [\theta(\bar{\vartheta} - \vartheta_m)]^{+}\frac{v^{d+1}_{i,j,l,m+1} - v^{d+1}_{i,j,l,m}}{\Delta \vartheta} + [\theta(\bar{\vartheta} - \vartheta_m)]^{-}\frac{v^{d+1}_{i,j,l,m} - v^{d+1}_{i,j,l,m-1}}{\Delta \vartheta} \\
&+ \frac{\vartheta_m \nu^2}{2}\frac{v^{d+1}_{i,j,l,m+1} - 2v^{d+1}_{i,j,l,m} + v^{d+1}_{i,j,l,m-1}}{(\Delta \vartheta)^2}.
\end{aligned}
\tag{B.6}
$$

Collecting terms with the same subscripts on the right-hand side yields

$$
\begin{aligned}
\frac{v^{d+1}_{i,j,l,m} - v^{d}_{i,j,l,m}}{\Delta} + \rho v^{d+1}_{i,j,l,m} =& \frac{(c^{d}_{i,j,l,m})^{1-\gamma}}{1-\gamma} + \frac{1}{2\varepsilon}(h^{d}_{i,j,l,m})^2 + v^{d+1}_{i-1,j,l,m}\alpha^{d}_{i,j,l,m} + v^{d+1}_{i,j,l,m}\beta^{d}_{i,j,l,m} \\
&+ v^{d+1}_{i+1,j,l,m}\zeta^{d}_{i,j,l,m} + v^{d+1}_{i,-j,l,m}\lambda_j \\
&+ v^{d+1}_{i,j,l-1,m}\alpha^{d}_{K,l,m} + v^{d+1}_{i,j,l+1,m}\zeta^{d}_{K,l,m} \\
&+ v^{d+1}_{i,j,l,m-1}\alpha^{d}_{\vartheta,m} + v^{d+1}_{i,j,l,m+1}\zeta^{d}_{\vartheta,m},
\end{aligned}
\tag{B.7}
$$

where

$$
\begin{aligned}
\alpha^d_{i,j,l,m} &= -\frac{[s^d_{i,j,l,m,B}]^-}{\Delta a} + \frac{\vartheta_m (k^d_{i,j,l,m})^2}{2(\Delta a)^2} \\
\beta^d_{i,j,l,m} &= -\frac{[s^d_{i,j,l,m,F}]^+}{\Delta a} + \frac{[s^d_{i,j,l,m,B}]^-}{\Delta a} - \lambda_j - \frac{\vartheta_m (k^d_{i,j,l,m})^2}{(\Delta a)^2} + \frac{[p^d_{l,m}]^-}{\Delta K} - \frac{[p^d_{l,m}]^+}{\Delta K} \\
&\quad + \frac{[\theta(\bar{\vartheta} - \vartheta_m)]^-}{\Delta \vartheta} - \frac{[\theta(\bar{\vartheta} - \vartheta_m)]^+}{\Delta \vartheta} - \frac{\vartheta_m \nu^2}{(\Delta \vartheta)^2} \\
\zeta^d_{i,j,l,m} &= \frac{[s^d_{i,j,l,m,F}]^+}{\Delta a} + \frac{\vartheta_m (k^d_{i,j,l,m})^2}{2(\Delta a)^2} \\
\alpha^d_{K,l,m} &= -\frac{[p^d_{l,m}]^-}{\Delta K} \\
\zeta^d_{K,l,m} &= \frac{[p^d_{l,m}]^+}{\Delta K} \\
\alpha^d_{\vartheta,m} &= -\frac{[\theta(\bar{\vartheta} - \vartheta_m)]^-}{\Delta \vartheta} + \frac{\vartheta_m \nu^2}{2(\Delta \vartheta)^2} \\
\zeta^d_{\vartheta,m} &= \frac{[\theta(\bar{\vartheta} - \vartheta_m)]^+}{\Delta \vartheta} + \frac{\vartheta_m \nu^2}{2(\Delta \vartheta)^2}
\end{aligned}
\tag{B.8}
$$

The discretized HJB equation (B.7) involves undefined terms $v^{d+1}_{0,j,l,m}$, $v^{d+1}_{I+1,j,l,m}$, $v^{d+1}_{i,j,0,m}$, $v^{d+1}_{i,j,L+1,m}$, $v^{d+1}_{i,j,l,0}$ and $v^{d+1}_{i,j,l,M+1}$. This calls for imposing some boundary conditions regarding both aggregate and individual states. The boundary conditions for aggregate states K and ϑ are based on reflections

$$
\partial_K v_{i,j,1,m} = \partial_K v_{i,j,L,m} = \partial_\vartheta v_{i,j,l,1} = \partial_\vartheta v_{i,j,l,M} = 0, \tag{B.9}
$$

implying $v^{d+1}_{i,j,0,m} = v^{d+1}_{i,j,1,m}$, $v^{d+1}_{i,j,L+1,m} = v^{d+1}_{i,j,L,m}$, $v^{d+1}_{i,j,l,0} = v^{d+1}_{i,j,l,1}$, and $v^{d+1}_{i,j,l,M+1} = v^{d+1}_{i,j,l,M}$.

The boundary conditions for the individual state a are specified as follows. At the lower bound a_1, we make use of the results that $k^d_{1,j,l,m} = h^d_{1,j,l,m} = 0$ and $s^d_{1,j,l,m,B} = \hat{s}^d_{1,j,l,m,B} = 0$ at the bound. Thus, $\alpha^d_{1,j,l,m} = 0$ and the term $v^{d+1}_{0,j,l,m}$ disappears. The treatment of the upper bound a_I is a bit more tricky. Similar to Achdou et al. (2022), we exploit the homogeneity properties of the value function as demonstrated in our stationary model. For large a, the function is of the form

$$
v_j(a) \approx x_0 a^{1-\gamma} + x_1 \varepsilon a^{2(1-\gamma)},
$$

where x_0 and x_1 are two known constants. Thus, $\partial_a v_j(a) \approx x_0(1-\gamma)a^{-\gamma} + x_1\varepsilon 2(1-\gamma)a^{1-2\gamma}$, $\partial_{aa} v_j(a) \approx x_0(1-\gamma)(-\gamma)a^{-\gamma-1} + x_1\varepsilon 2(1-\gamma)(1-2\gamma)a^{-2\gamma}$. Assuming $\gamma > 1$

gives

$$\lim_{a\to\infty}\frac{\partial_{aa}v_j(a)a}{-\gamma\partial_a v_j(a)}\approx\lim_{a\to\infty}\frac{x_0(1-\gamma)a^{-\gamma}+x_1\varepsilon 2(-\gamma^{-1}+1)(1-2\gamma)a^{1-2\gamma}}{x_0(1-\gamma)a^{-\gamma}+x_1\varepsilon 2(1-\gamma)a^{1-2\gamma}}$$
$$=\lim_{a\to\infty}\frac{x_0(1-\gamma)+x_1\varepsilon 2(-\gamma^{-1}+1)(1-2\gamma)a^{1-\gamma}}{x_0(1-\gamma)+x_1\varepsilon 2(1-\gamma)a^{1-\gamma}}=1.$$

Consequently, this motivates the following approximations at the upper bound a_I as

$$\partial_{aa}v_{I,j,l,m}=-\frac{\gamma\partial_a v_{I,j,l,m}}{a_I}, k_{I,j,l,m}=-\frac{\pi_{I,j,l,m}}{\vartheta_m}\frac{\partial_a v_{I,j,l,m}}{\partial_{aa}v_{I,j,l,m}}=\frac{\pi_{I,j,l,m}}{\gamma\vartheta_m}a_I,$$

and then

$$\frac{\vartheta_m(k_{I,j,l,m})^2}{2}\partial_{aa}v_{I,j,l,m}=-\frac{\pi^2_{I,j,l,m}a_I}{2\gamma\vartheta_m}\partial_a v_{I,j,l,m}. \tag{B.10}$$

Here the perceived excess return at a_I equals

$$\pi_{I,j,l,m}=R_{l,m}-r_{l,m}+\sqrt{\vartheta_m}h_{I,j,l,m}\approx(R_{l,m}-r_{l,m})\left(1-\varepsilon\frac{\alpha_0}{\gamma\sqrt{\vartheta_m}}a_I^{1-\gamma}\right), \tag{B.11}$$

where α_0 is given in (A.69) with $\sigma=\sqrt{\vartheta_m}$. Substituting (B.10) into (B.2) gives

$$\begin{aligned}\frac{v^{d+1}_{I,j,l,m}-v^d_{I,j,l,m}}{\Delta}+\rho v^{d+1}_{I,j,l,m}=&\frac{(c^d_{I,j,l,m})^{1-\gamma}}{1-\gamma}+\frac{1}{2\varepsilon}(h^d_{I,j,l,m})^2+[s^d_{I,j,l,m,F}]^+\frac{v^{d+1}_{I+1,j,l,m}-v^{d+1}_{I,j,l,m}}{\Delta a}\\&+[s^d_{I,j,l,m,B}]^-\frac{v^{d+1}_{I,j,l,m}-v^{d+1}_{I-1,j,l,m}}{\Delta a}+\lambda_j(v^{d+1}_{I,-j,l,m}-v^{d+1}_{I,j,l,m})\\&-\frac{(\pi^d_{I,j,l,m})^2a_I}{2\gamma\vartheta_m}\frac{v^{d+1}_{I,j,l,m}-v^{d+1}_{I-1,j,l,m}}{\Delta a}\\&+[p_{l,m}]^+\frac{v^{d+1}_{I,j,l+1,m}-v^{d+1}_{I,j,l,m}}{\Delta K}+[p_{l,m}]^-\frac{v^{d+1}_{I,j,l,m}-v^{d+1}_{I,j,l-1,m}}{\Delta K}\\&+[\theta(\bar\vartheta-\vartheta_m)]^+\frac{v^{d+1}_{I,j,l,m+1}-v^{d+1}_{I,j,l,m}}{\Delta\vartheta}+[\theta(\bar\vartheta-\vartheta_m)]^-\frac{v^{d+1}_{I,j,l,m}-v^{d+1}_{I,j,l,m-1}}{\Delta\vartheta}\\&+\frac{\vartheta_m\nu^2}{2}\frac{v^{d+1}_{I,j,l,m+1}-2v^{d+1}_{I,j,l,m}+v^{d+1}_{I,j,l,m-1}}{(\Delta\vartheta)^2}.\end{aligned} \tag{B.12}$$

Collecting terms with the same subscripts on the right-hand side yields

$$\begin{aligned}\frac{v^{d+1}_{I,j,l,m}-v^{d}_{I,j,l,m}}{\Delta}+\rho v^{d+1}_{I,j,l,m}=&\frac{(c^{d}_{I,j,l,m})^{1-\gamma}}{1-\gamma}+\frac{1}{2\varepsilon}(h^{d}_{I,j,l,m})^{2}+v^{d+1}_{I-1,j,l,m}\alpha^{d}_{I,j,l,m}+v^{d+1}_{I,j,l,m}\beta^{d}_{I,j,l,m}\\&+v^{d+1}_{I+1,j,l,m}\xi^{d}_{I,j,l,m}+v^{d+1}_{I,-j,l,m}\lambda_{j}\\&+v^{d+1}_{I,j,l-1,m}\alpha^{d}_{K,l,m}+v^{d+1}_{I,j,l+1,m}\xi^{d}_{K,l,m}\\&+v^{d+1}_{I,j,l,m-1}\alpha^{d}_{\vartheta,m}+v^{d+1}_{I,j,l,m+1}\xi^{d}_{\vartheta,m},\end{aligned}\tag{B.13}$$

where

$$\begin{aligned}\alpha^{d}_{I,j,l,m}&=-\frac{[s^{d}_{I,j,l,m,B}]^{-}}{\Delta a}+\frac{(\pi^{d}_{I,j,l,m})^{2}a_{I}}{2\gamma\vartheta_{m}\Delta a}\\\beta^{d}_{I,j,l,m}&=-\frac{[s^{d}_{I,j,l,m,F}]^{+}}{\Delta a}+\frac{[s^{d}_{I,j,l,m,B}]^{-}}{\Delta a}-\lambda_{j}-\frac{(\pi^{d}_{I,j,l,m})^{2}a_{I}}{2\gamma\vartheta_{m}\Delta a}+\frac{[p^{d}_{l,m}]^{-}}{\Delta K}-\frac{[p^{d}_{l,m}]^{+}}{\Delta K}\\&\quad+\frac{[\theta(\bar{\vartheta}-\vartheta_{m})]^{-}}{\Delta\vartheta}-\frac{[\theta(\bar{\vartheta}-\vartheta_{m})]^{+}}{\Delta\vartheta}-\frac{\vartheta_{m}\nu^{2}}{(\Delta\vartheta)^{2}}\\\xi^{d}_{I,j,l,m}&=\frac{[s^{d}_{I,j,l,m,F}]^{+}}{\Delta a}\end{aligned}\tag{B.14}$$

At a_I, we impose a state constraint $a \le a_I$ by setting $s^{d}_{I,j,l,m,F}=0$. Thus, $\xi^{d}_{I,j,l,m}=0$ and the term $v^{d+1}_{I+1,j,l,m}$ is never used.

To sum up, we convert the approximate HJB equations (B.7) and (B.13) into a system of $I\times 2\times L\times N$ nonlinear equations as

$$\frac{1}{\Delta}(\mathbf{v}^{d+1}-\mathbf{v}^{d})+\rho\mathbf{v}^{d+1}=\mathbf{u}^{d}+\mathbf{A}^{d}\mathbf{v}^{d+1}\Leftrightarrow\mathbf{B}^{d}\mathbf{v}^{d+1}=\mathbf{d}^{d},\tag{B.15}$$

where $\mathbf{B}^{d}=(\frac{1}{\Delta}+\rho)\mathbf{I}-\mathbf{A}^{d}$ and $\mathbf{d}^{d}=\mathbf{u}^{d}+\frac{1}{\Delta}\mathbf{v}^{d}$. Solving equation (B.15) iteratively yields the desired value and policy functions. In the equation, the vectors $\mathbf{v}^{d+1}$ and $\mathbf{u}^{d}$, and the matrix $\mathbf{A}^{d}$ are defined as follows: $\forall\, l=1,\cdots,L,\ m=1,\cdots,M$, denote

$$\mathbf{v}^{d+1}_{l,m}=\begin{bmatrix}\mathbf{v}^{d+1}_{1,1,l,m}\\\vdots\\\mathbf{v}^{d+1}_{I,1,l,m}\\\mathbf{v}^{d+1}_{1,2,l,m}\\\vdots\\\mathbf{v}^{d+1}_{I,2,l,m}\end{bmatrix},\ \mathbf{v}^{d+1}_{m}=\begin{bmatrix}\mathbf{v}^{d+1}_{1,m}\\\mathbf{v}^{d+1}_{2,m}\\\vdots\\\mathbf{v}^{d+1}_{L,m}\end{bmatrix},\ \mathbf{v}^{d+1}=\begin{bmatrix}\mathbf{v}^{d+1}_{1}\\\mathbf{v}^{d+1}_{2}\\\vdots\\\mathbf{v}^{d+1}_{M}\end{bmatrix},\tag{B.16}$$

$$\mathbf{u}^d_{l,m} = \begin{bmatrix} \frac{(c^d_{1,1,l,m})^{1-\gamma}}{1-\gamma} + \frac{(h^d_{1,1,l,m})^2}{2\varepsilon} \\ \vdots \\ \frac{(c^d_{I,1,l,m})^{1-\gamma}}{1-\gamma} + \frac{(h^d_{I,1,l,m})^2}{2\varepsilon} \\ \frac{(c^d_{1,2,l,m})^{1-\gamma}}{1-\gamma} + \frac{(h^d_{1,2,l,m})^2}{2\varepsilon} \\ \vdots \\ \frac{(c^d_{I,2,l,m})^{1-\gamma}}{1-\gamma} + \frac{(h^d_{I,2,l,m})^2}{2\varepsilon} \end{bmatrix}, \ \mathbf{u}^d_m = \begin{bmatrix} \mathbf{u}^d_{1,m} \\ \mathbf{u}^d_{2,m} \\ \vdots \\ \mathbf{u}^d_{L,m} \end{bmatrix}, \ \mathbf{u}^d = \begin{bmatrix} \mathbf{u}^d_1 \\ \mathbf{u}^d_2 \\ \vdots \\ \mathbf{u}^d_M \end{bmatrix}, \tag{B.17}$$

$$\mathbf{A}^d_{l,m} = \begin{bmatrix} \beta^d_{1,1,l,m} & \xi^d_{1,1,l,m} & 0 & \cdots & 0 & \lambda_1 & 0 & 0 & \cdots & 0 \\ \alpha^d_{2,1,l,m} & \beta^d_{2,1,l,m} & \xi^d_{2,1,l,m} & 0 & \cdots & 0 & \lambda_1 & 0 & 0 & \cdots \\ 0 & \alpha^d_{3,1,l,m} & \beta^d_{3,1,l,m} & \xi^d_{3,1,l,m} & \cdots & 0 & 0 & \lambda_1 & 0 & \cdots \\ \vdots & \ddots & \ddots & \ddots & \ddots & \ddots & \ddots & \ddots & \ddots & \vdots \\ 0 & \cdots & 0 & \alpha^d_{I,1,l,m} & \beta^d_{I,1,l,m} & 0 & 0 & \cdots & 0 & \lambda_1 \\ \lambda_2 & 0 & 0 & \cdots & 0 & \beta^d_{1,2,l,m} & \xi^d_{1,2,l,m} & 0 & \cdots & 0 \\ 0 & \lambda_2 & 0 & 0 & \cdots & \alpha^d_{2,2,l,m} & \beta^d_{2,2,l,m} & \xi^d_{2,2,l,m} & 0 & \cdots \\ 0 & 0 & \lambda_2 & 0 & \cdots & 0 & \alpha^d_{3,2,l,m} & \beta^d_{3,2,l,m} & \xi^d_{3,2,l,m} & \cdots \\ \vdots & \ddots & \ddots & \ddots & \ddots & \ddots & \ddots & \ddots & \ddots & \vdots \\ 0 & 0 & \cdots & 0 & \lambda_2 & 0 & \cdots & 0 & \alpha^d_{I,2,l,m} & \beta^d_{I,2,l,m} \end{bmatrix}, \tag{B.18}$$

$$\mathbf{A}^d_m = \begin{bmatrix} \mathbf{A}^d_{1,m} + \alpha^d_{K,1,m}\mathbf{I}_{2I} & \xi^d_{K,1,m}\mathbf{I}_{2I} & \mathbf{0}_{2I} & \mathbf{0}_{2I} & \cdots & \mathbf{0}_{2I} \\ \alpha^d_{K,2,m}\mathbf{I}_{2I} & \mathbf{A}^d_{2,m} & \xi^d_{K,2,m}\mathbf{I}_{2I} & \mathbf{0}_{2I} & \cdots & \mathbf{0}_{2I} \\ \mathbf{0}_{2I} & \alpha^d_{K,3,m}\mathbf{I}_{2I} & \mathbf{A}^d_{3,m} & \xi^d_{K,3,m}\mathbf{I}_{2I} & \cdots & \mathbf{0}_{2I} \\ \vdots & \ddots & \ddots & \ddots & \ddots & \vdots \\ \mathbf{0}_{2I} & \cdots & \cdots & \alpha^d_{K,L-1,m}\mathbf{I}_{2I} & \mathbf{A}^d_{L-1,m} & \xi^d_{K,L-1,m}\mathbf{I}_{2I} \\ \mathbf{0}_{2I} & \cdots & \cdots & \mathbf{0}_{2I} & \alpha^d_{K,L,m}\mathbf{I}_{2I} & \mathbf{A}^d_{L,m} + \xi^d_{K,L,m}\mathbf{I}_{2I} \end{bmatrix}, \tag{B.19}$$

$$
\mathbf{A}^d = \begin{bmatrix}
\mathbf{A}_1^d + \alpha_{\vartheta,1}^d \mathbf{I}_{2I\times L} & \xi_{\vartheta,1}^d \mathbf{I}_{2I\times L} & \mathbf{0}_{2I\times L} & \mathbf{0}_{2I\times L} & \cdots & \mathbf{0}_{2I\times L} \\
\alpha_{\vartheta,2}^d \mathbf{I}_{2I\times L} & \mathbf{A}_2^d & \xi_{\vartheta,2}^d \mathbf{I}_{2I\times L} & \mathbf{0}_{2I\times L} & \cdots & \mathbf{0}_{2I\times L} \\
\mathbf{0}_{2I\times L} & \alpha_{\vartheta,3}^d \mathbf{I}_{2I\times L} & \mathbf{A}_3^d & \xi_{\vartheta,3}^d \mathbf{I}_{2I\times L} & \cdots & \mathbf{0}_{2I\times L} \\
\vdots & \ddots & \ddots & \ddots & \ddots & \vdots \\
\mathbf{0}_{2I\times L} & \cdots & \cdots & \alpha_{\vartheta,M-1}^d \mathbf{I}_{2I\times L} & \mathbf{A}_{M-1}^d & \xi_{\vartheta,M-1}^d \mathbf{I}_{2I\times L} \\
\mathbf{0}_{2I\times L} & \cdots & \cdots & \mathbf{0}_{2I\times L} & \alpha_{\vartheta,M}^d \mathbf{I}_{2I\times L} & \mathbf{A}_M^d + \xi_{\vartheta,M}^d \mathbf{I}_{2I\times L}
\end{bmatrix}. \tag{B.20}
$$

B.2 Solving the KF equation

Let $g_{t,i,j,l,m} = g_t(a_i, z_j | K_l, \vartheta_m)$ be the density conditional on the time-t aggregate state of $K_t = K_l$ and $\vartheta_t = \vartheta_m$. The KF equation (2.15) can be written as

$$
\frac{\partial}{\partial t} g_{t,i,j,l,m} = -\frac{\partial}{\partial a}\left(\hat{s}_{i,j,l,m} g_{t,i,j,l,m}\right) - \lambda_j g_{t,i,i,l,m} + \lambda_{-j} g_{t,i,-j,l,m} + \frac{1}{2}\frac{\partial^2}{\partial a^2}\left(\vartheta_m (k_{i,j,l,m})^2 g_{t,i,j,l,m}\right). \tag{B.21}
$$

It is worth noting that the saving function used the above equation corresponds to the actual saving $\hat{s}$ not the perceived saving s. More precisely, $\hat{s}_{i,j,l,m} = s_{i,j,l,m} + \sqrt{\vartheta_m} h_{i,j,l,m}$. Therefore, as opposed to the existing literature, when computing the KF equation, we cannot actually use the $\mathbf{A}$ matrix "for free" without proper adjustments.

Let Δt be the time step. We discretize the KF equation (B.21) as

$$
\begin{aligned}
\frac{g_{t+1,i,j,l,m} - g_{t,i,j,l,m}}{\Delta t} = &- \frac{\left[\hat{s}_{i,j,l,m,F}\right]^+ g_{t+1,i,j,l,m} - \left[\hat{s}_{i-1,j,l,m,F}\right]^+ g_{t+1,i-1,j,l,m}}{\Delta a} \\
&- \frac{\left[\hat{s}_{i+1,j,l,m,B}\right]^- g_{t+1,i+1,j,l,m} - \left[\hat{s}_{i,j,l,m,B}\right]^- g_{t+1,i,j,l,m}}{\Delta a} \\
&- \lambda_j g_{t+1,i,i,l,m} + \lambda_{-j} g_{t+1,i,-j,l,m} \\
&+ \frac{\vartheta_m}{2} \frac{k_{i+1,j,l,m}^2 g_{t+1,i+1,j,l,m} - 2k_{i,j,l,m}^2 g_{t+1,i,j,l,m} + k_{i-1,j,l,m}^2 g_{t+1,i-1,j,l,m}}{(\Delta a)^2}.
\end{aligned} \tag{B.22}
$$

Collecting terms, equation (B.22) can be written as

$$
\frac{g_{t+1,i,j,l,m} - g_{t,i,j,l,m}}{\Delta t} = \hat{\xi}_{i-1,j,l,m} g_{t+1,i-1,j,l,m} + \hat{\beta}_{i,j,l,m} g_{t+1,i,j,l,m} + \hat{\alpha}_{i+1,j,l,m} g_{t+1,i+1,j,l,m} + \lambda_{-j} g_{t,i,-j,l,m}. \tag{B.23}
$$

Here the coefficients are

$$
\begin{aligned}
\hat{\alpha}_{i,j,l,m} &= -\frac{[\hat{s}_{i,j,l,m,B}]^-}{\Delta a} + \frac{\vartheta_n (k_{i,j,l,m})^2}{2(\Delta a)^2} = \alpha_{i,j,l,m} + \Delta\alpha_{i,j,l,m} \\
\hat{\beta}_{i,j,l,m} &= -\frac{[\hat{s}_{i,j,l,m,F}]^+}{\Delta a} + \frac{[\hat{s}_{i,j,l,m,B}]^-}{\Delta a} - \lambda_j - \frac{\vartheta_m (k_{i,j,l,m})^2}{(\Delta a)^2} = \beta_{i,j,l,m} + \Delta\xi_{i,j,l,m} \\
\hat{\xi}_{i,j,l,m} &= \frac{[\hat{s}_{i,j,l,m,F}]^+}{\Delta a} + \frac{\vartheta_m (k_{i,j,l,m})^2}{2(\Delta a)^2} = \xi_{i,j,l,m} + \Delta\xi_{i,j,l,m},
\end{aligned}
\tag{B.24}
$$

where $\alpha_{i,j,l,m}$, $\beta_{i,j,l,m}$, and $\xi_{i,j,l,m}$ are given in (B.8), and

$$
\begin{aligned}
\Delta\alpha_{i,j,l,m} &= \frac{[s_{i,j,l,m,B}]^-}{\Delta a} - \frac{[\hat{s}_{i,j,l,m,B}]^-}{\Delta a} \\
\Delta\beta_{i,j,l,m} &= \left(\frac{[\hat{s}_{i,j,l,m,B}]^-}{\Delta a} - \frac{[s_{i,j,l,m,B}]^-}{\Delta a}\right) + \left(\frac{[s_{i,j,l,m,F}]^+}{\Delta a} - \frac{[\hat{s}_{i,j,l,m,F}]^+}{\Delta a}\right) \\
&\quad - \frac{[p^d_{l,m}]^-}{\Delta K} + \frac{[p^d_{l,m}]^+}{\Delta K} - \frac{[\theta(\bar{\vartheta} - \vartheta_m)]^-}{\Delta\vartheta} + \frac{[\theta(\bar{\vartheta} - \vartheta_m)]^+}{\Delta\vartheta} + \frac{\vartheta_m \nu^2}{(\Delta\vartheta)^2} \\
\Delta\xi_{i,j,l,m} &= \frac{[\hat{s}_{i,j,l,m,F}]^+}{\Delta a} - \frac{[s_{i,j,l,m,F}]^+}{\Delta a}.
\end{aligned}
\tag{B.25}
$$

Note that $\Delta\alpha_{i,j,l,m}$, $\Delta\beta_{i,j,l,m}$, and $\Delta\xi_{i,j,l,m}$ are in general different from zero because of the disparity between actual and perceived saving rates. For $\Delta\beta_{i,j,l,m}$, the discrepancy also arises from the effects of the evolution of aggregate states, i.e., $-\frac{[p^d_{l,m}]^-}{\Delta K} + \frac{[p^d_{l,m}]^+}{\Delta K} - \frac{[\theta(\bar{\vartheta}-\vartheta_m)]^-}{\Delta\vartheta} + \frac{[\theta(\bar{\vartheta}-\vartheta_m)]^+}{\Delta\vartheta} + \frac{\vartheta_m \nu^2}{(\Delta\vartheta)^2}$, which are directly taken into account by households in the HJB equation but not so in the KF equation.

The approximate KF equations (B.23) can be written in the following matrix form:

$$
\frac{\mathbf{g}_{t+1} - \mathbf{g}_t}{\Delta t} = \hat{\mathbf{A}}^T_{l,m}\mathbf{g}_t \Leftrightarrow \mathbf{g}_{t+1} = (\mathbf{I} - \Delta t \hat{\mathbf{A}}^T_{l,m})^{-1}\mathbf{g}_t,
\tag{B.26}
$$

where

$$
\mathbf{g}_t = \begin{bmatrix} \mathbf{g}_{t,1,1,l,m} \\ \vdots \\ \mathbf{g}_{t,I,1,l,m} \\ \mathbf{g}_{t,1,2,l,m} \\ \vdots \\ \mathbf{g}_{t,I,2,l,m} \end{bmatrix},
\tag{B.27}
$$

$$\hat{\mathbf{A}}_{l,m} = \begin{bmatrix} \hat{\beta}_{1,1,l,m} & \hat{\xi}_{1,1,l,m} & 0 & \cdots & 0 & \lambda_1 & 0 & 0 & \cdots & 0 \\ \hat{\alpha}_{2,1,l,m} & \hat{\beta}_{2,1,l,m} & \hat{\xi}_{2,1,l,m} & 0 & \cdots & 0 & \lambda_1 & 0 & 0 & \cdots \\ 0 & \hat{\alpha}_{3,1,l,m} & \hat{\beta}_{3,1,l,m} & \hat{\xi}_{3,1,l,m} & \cdots & 0 & 0 & \lambda_1 & 0 & \cdots \\ \vdots & \ddots & \ddots & \ddots & \ddots & \ddots & \ddots & \ddots & \ddots & \vdots \\ 0 & \cdots & 0 & \hat{\alpha}_{I,1,l,m} & \hat{\beta}_{I,1,l,m} & 0 & 0 & \cdots & 0 & \lambda_1 \\ \lambda_2 & 0 & 0 & \cdots & 0 & \hat{\beta}_{1,2,l,m} & \hat{\xi}_{1,2,l,m} & 0 & \cdots & 0 \\ 0 & \lambda_2 & 0 & 0 & \cdots & \hat{\alpha}_{2,2,l,m} & \hat{\beta}_{2,2,l,m} & \hat{\xi}_{2,2,l,m} & 0 & \cdots \\ 0 & 0 & \lambda_2 & 0 & \cdots & 0 & \hat{\alpha}_{3,2,l,m} & \hat{\beta}_{3,2,l,m} & \hat{\xi}_{3,2,l,m} & \cdots \\ \vdots & \ddots & \ddots & \ddots & \ddots & \ddots & \ddots & \ddots & \ddots & \vdots \\ 0 & 0 & \cdots & 0 & \lambda_2 & 0 & \cdots & 0 & \hat{\alpha}_{I,2,l,m} & \hat{\beta}_{I,2,l,m} \end{bmatrix}. \tag{B.28}$$

Again, as discussed previously, $\hat{\mathbf{A}}_{l,m} \neq \mathbf{A}_{l,m} = \lim_{d\to\infty} \mathbf{A}^d_{l,m}$ in general.

C Data sources

We collected the following aggregate time series from the St.Louis FED - FRED database (mnemonics in parentheses). These series are quarterly frequency from 1984Q1 to 2019Q4.

Per-capita output.

1. Per-capita real gross domestic product (A939RX0Q048SBEA)
2. Source: St.Louis FED - FRED database

Per-capita investment.

1. Per-capita real personal consumption expenditures on durable goods (A795RX0Q048SBEA)
2. + Real Gross Private Domestic Investment (GPDIC1) /Population (CNP16OV)
3. Source: St.Louis FED - FRED database

Per-capita consumption.

1. Per-capita real personal consumption expenditures on nondurable goods (A796RX0Q048SBEA)
2. + services (A797RX0Q048SBEA)
3. Source: St.Louis FED - FRED database

TFP.

1. Fernald (2014)

2. Source: https://www.johnfernald.net/TFP

D Additional figures

Figure 7: Effects of risk shock on aggregate variables by investment risk level

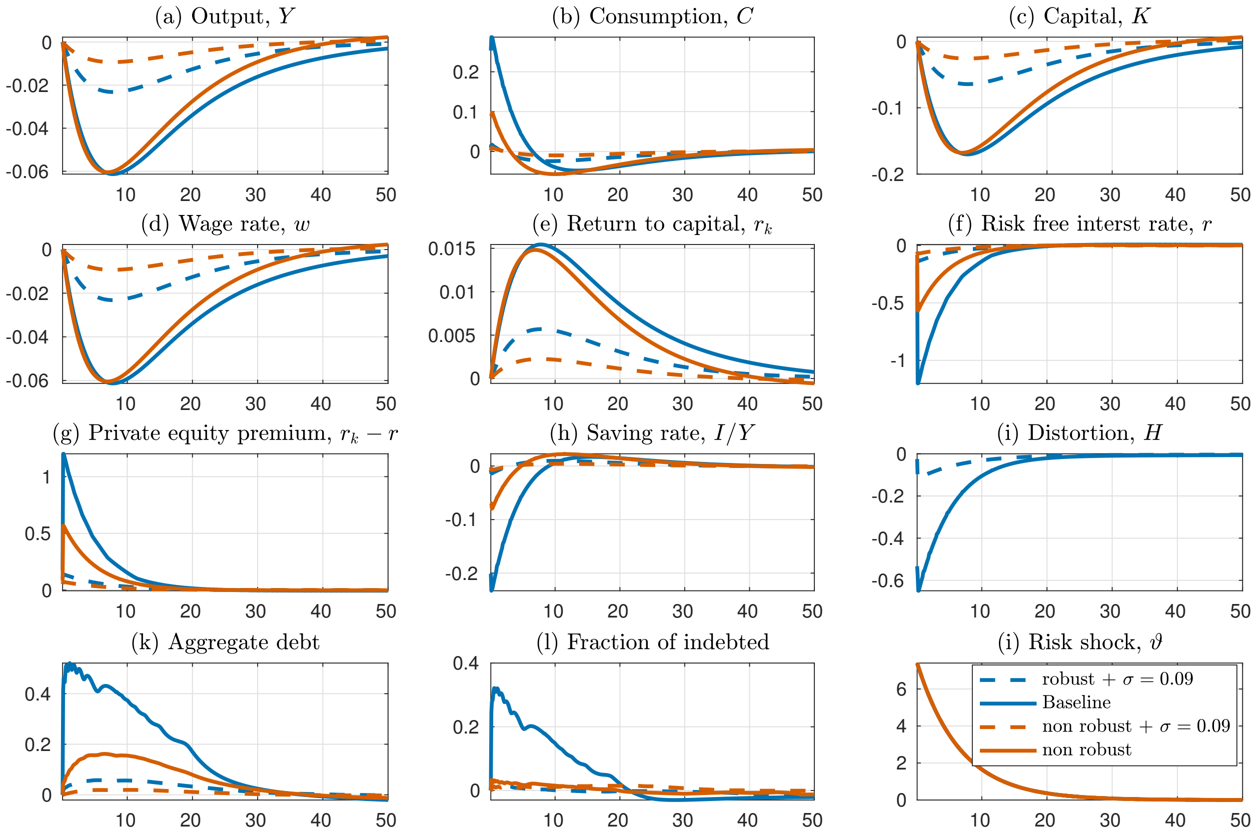

Notes: Panel (k) reports aggregate debt defined as $\frac{B}{K} = \frac{\int_{b<=0} bdG(a,z)}{K}$ and panel (l) shows the fraction of indebted households given by $\int_{b<=0} dG(a,z)$

Figure 8: Effects of risk shock on group-specific average by investment risk level

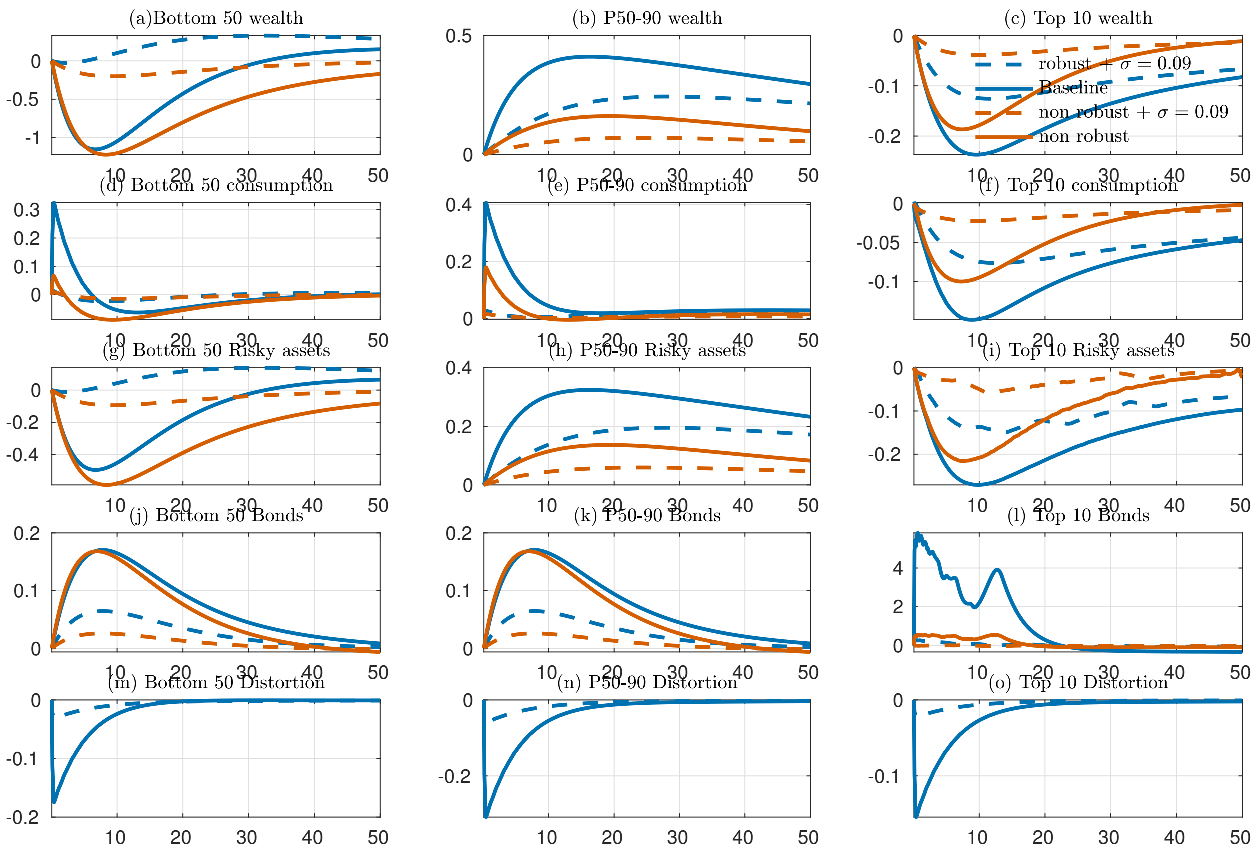

Figure 9: Effects of risk shock on wealth inequality by investment risk level

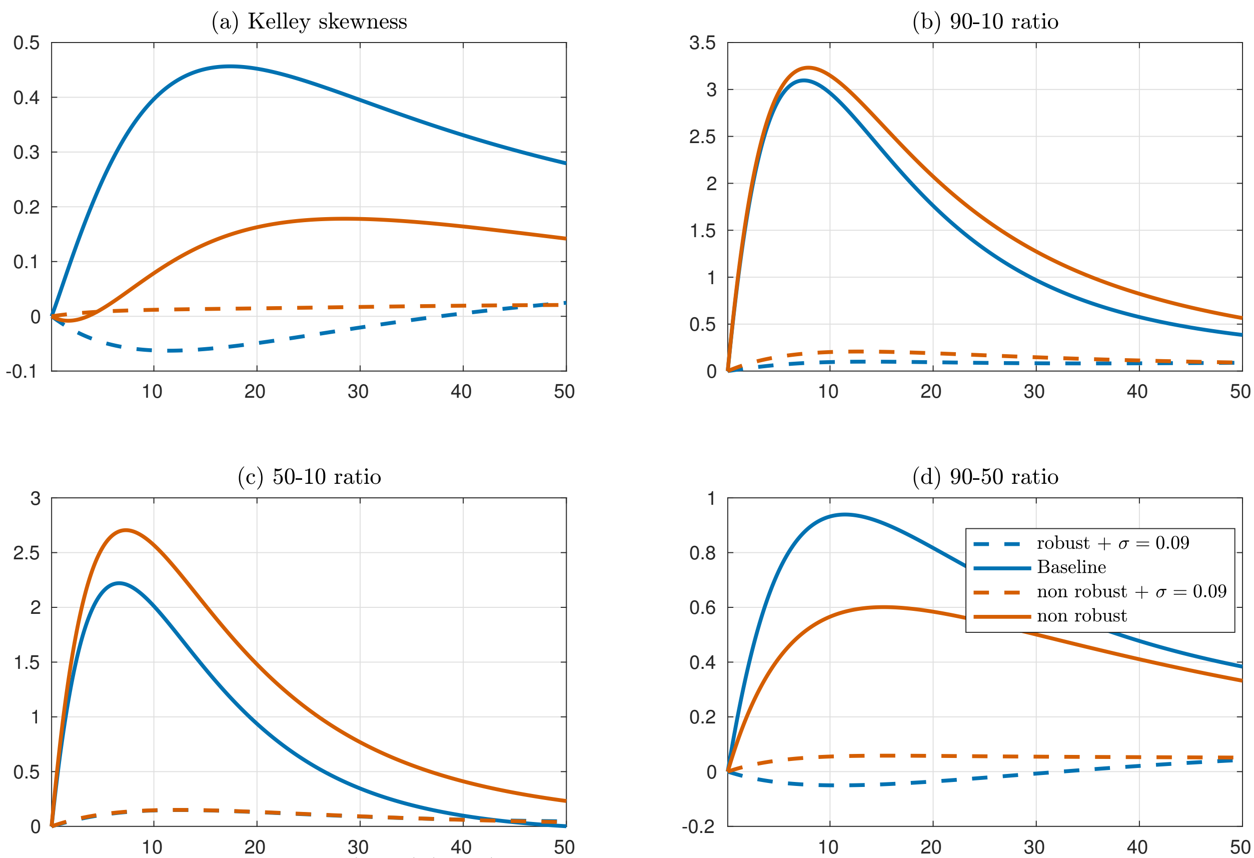

Notes: The Kelley measure is defined as : $SK = \frac{(P90-P50)-(P50-P10)}{P90-P10}$. A negative value indicates that the left-tail contribution to the overall dispersion is larger than that of the right tail.

Figure 10: Effects of risk and TFP shocks on aggregate variables

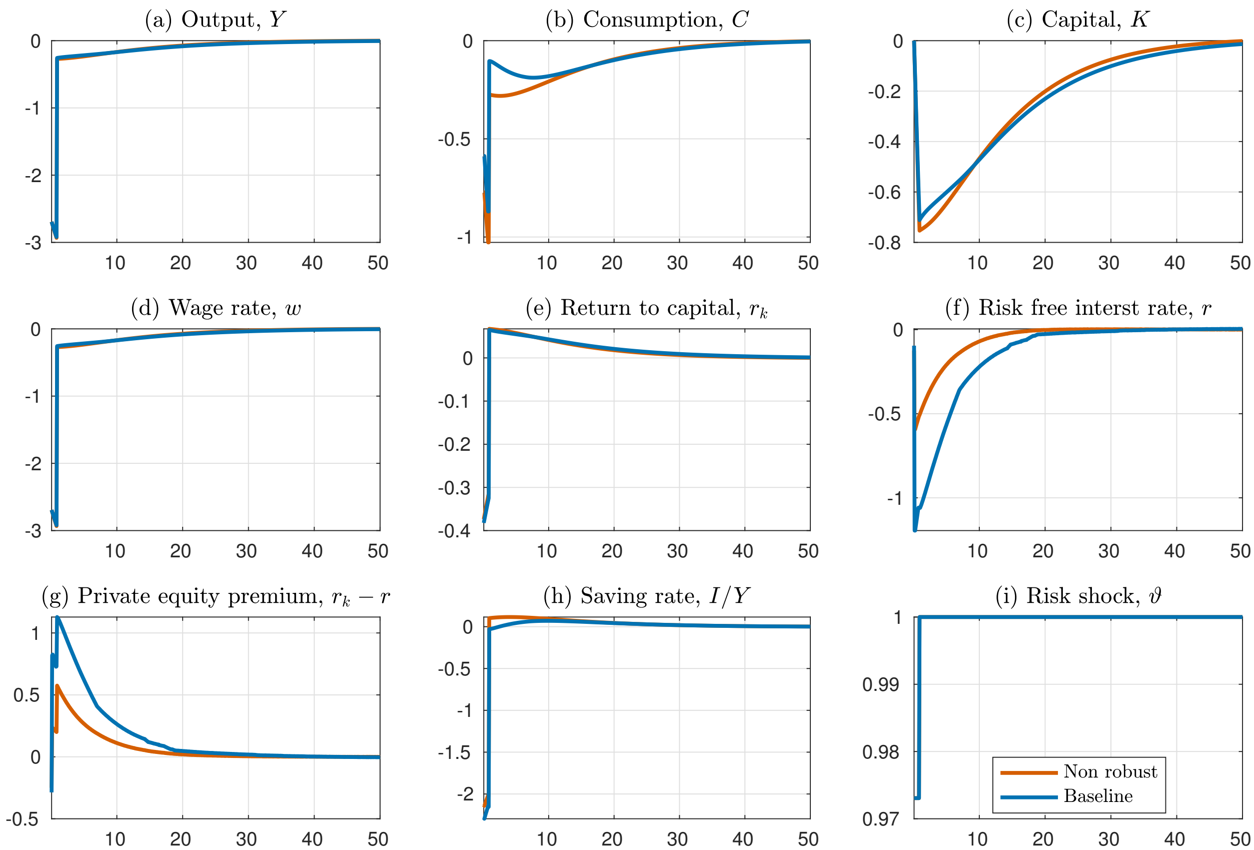

Figure 11: Effects of risk and TFP shocks on group-specific average

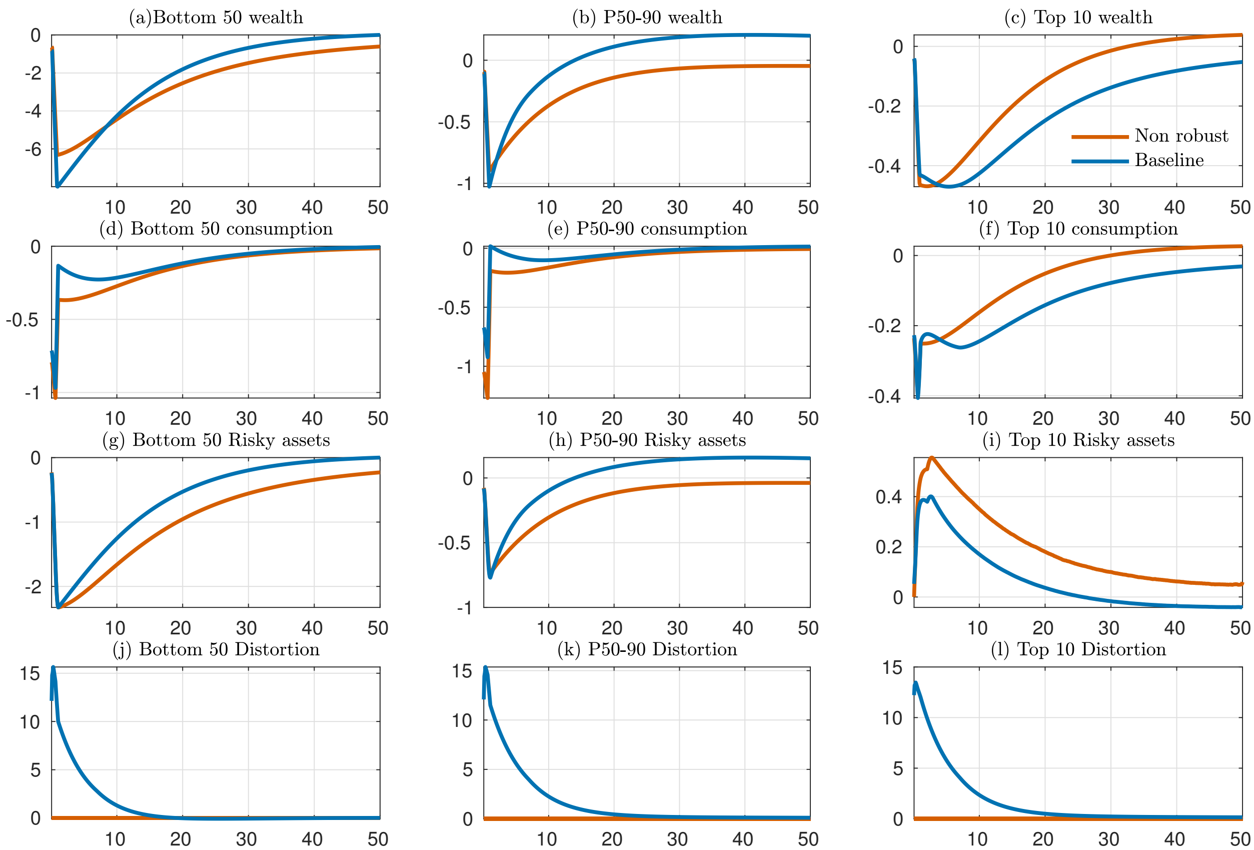

Figure 12: Effects of risk and TFP shocks on wealth inequality